

## Detailed response to the Reviewers' comments

We thank the Anonymous Reviewer #1 and Anonymous Reviewer #2 for the time devoted on reading and commenting the manuscript and the important suggestions for improvements. We address each comment given by the reviewers below.

All our additions and changes made in the manuscript are listed by chapters, pages and lines in the reply letter and marked in yellow in revised manuscript. In addition, changes (in italic) are pasted in below each reply to the reviewers (in most cases).

\*reviewer comment are in black and answers to those comments are in blue

### **Anonymous Reviewer #1**

The paper present novel data on modern and fossil planktic foraminifera in the southwestern Svalbard margin. Planktic foraminifera can be sensitive indicators of the changing Arctic environments. Living planktic foraminifera were collected at different vertical depth-sampling intervals in October 2012 and July 2014 at the coring site. The short (30.5 cm length sampled at 0.5 cm intervals) sediment core was collected in Storfjorden Fan at 1520 m water depth in October 2012 for fossil foraminifera studying. The environmental reconstructions (first of all sea surface temperatures) over the SW Svalbard margin are within the scope of CP. The paper is technically sound. The paper contains the novel and interesting research of the planktic foraminifera and structure of surface water masses at the SW Svalbard margin in relation to climate changes during the last 2000 years. Conclusions in the paper correspond to the objectives stated in the Introduction. The claims fully supported by the experimental data. The research was carried out at a sufficiently high scientific level. The authors provided sufficient methodological details that the methods could be reproduced.

I think the phrase “Trace element ratios of Mg/Ca and Al/Ca” on the page 7 may be replaced by “Elemental ratios of Mg/Ca and Al/Ca”

We thank Reviewer#1 for the kind and positive comments. We have replaced the phrase “Trace element ratios of Mg/Ca and Al/Ca” by “*Elemental ratios of Mg/Ca and Al/Ca*” as requested, p. 8, line 7.

---

There are enough data for providing the age model based on six  $^{14}\text{C}$  dates and  $^{210}\text{Pb}$  and  $^{137}\text{Cs}$  dating as well. The authors clearly indicate their own original contribution into relevant scientific questions. The list of references is quite huge. But I would like to see author's comments about their own sedimentation rates data and climatic inferences in the focus of previous related papers on Svalbard margin (Winkelmann, Knies, 2005; Pathirana et al., 2014, 2015; Vare et al., 2010 and so on).

We thank the Reviewer#1 for this suggestion and indication of relevant publications. Based on the pointed out studies we added a comment on our sedimentation rates data with references in chapter Results, 3.2.1, p. 12, lines 28-31:

*“These rates are similar to sedimentation rate reported for the Barents Sea which range from 0.06–0.09 cm yr<sup>-1</sup> to 0.10–0.14 cm yr<sup>-1</sup> dependent on whether the upper mixed layer is included in the calculations or not, respectively (Maiti et al., 2010; Vare et al., 2010; Pathirana et al., 2014; 2015 and references therein).”*

---

The authors made their paleoceanographical reconstructions based on one short core collected in Storfjorden Fan (SW Svalbard margin). More than 40 short cores were collected west off Svalbard and on the adjacent shelf to the south. I think the results of these studies should be reflected in the Introduction and in the Discussion of the paper.

Cited papers:

1. Pathirana, I., Knies, J., Felix, M., Mann, U. (2014) Towards an improved organic carbon budget for the western Barents Sea shelf, *Clim. Past*, 10, 569-587, <https://doi.org/10.5194/cp-10-569-2014>.
2. Pathirana I, Knies J, Felix M, Mann U, Ellingsen I (2015) Middle to late Holocene paleoproductivity reconstructions for the western Barents Sea: a model-data comparison, *Arktos* (2015) 1:20. doi: 10.1007/s41063-015-0002-z
3. Winkelmann D., Knies J. (2005) Recent distribution and accumulation of organic carbon on the continental margin west off Spitsbergen, *Geochem. Geophys. Geosyst.*, 6, Q09012, doi:10.1029/2005GC000916.
4. Vare LL, Masse G, Belt ST (2010) A biomarker-based reconstruction of sea ice conditions for the Barents Sea in recent centuries. *Holocene* 20:637–643. doi:10.1177/0959683609355179

We have followed the reviewer's suggestion and included the results of the suggested publications in the introduction (p. 2, line 15 and 25; p. 4, line 12-15), discussion section and the new chapter 4.3 Comparison to other studies (p. 21-23).

---

The title of the paper reflects the researches results and the contents of the paper. I think the abstract provide a concise and complete summary. I suppose the presentation is well structured and clear. The language is quite fluent but sometimes probably not precise. Please bear in mind that I am not a native English speaker.

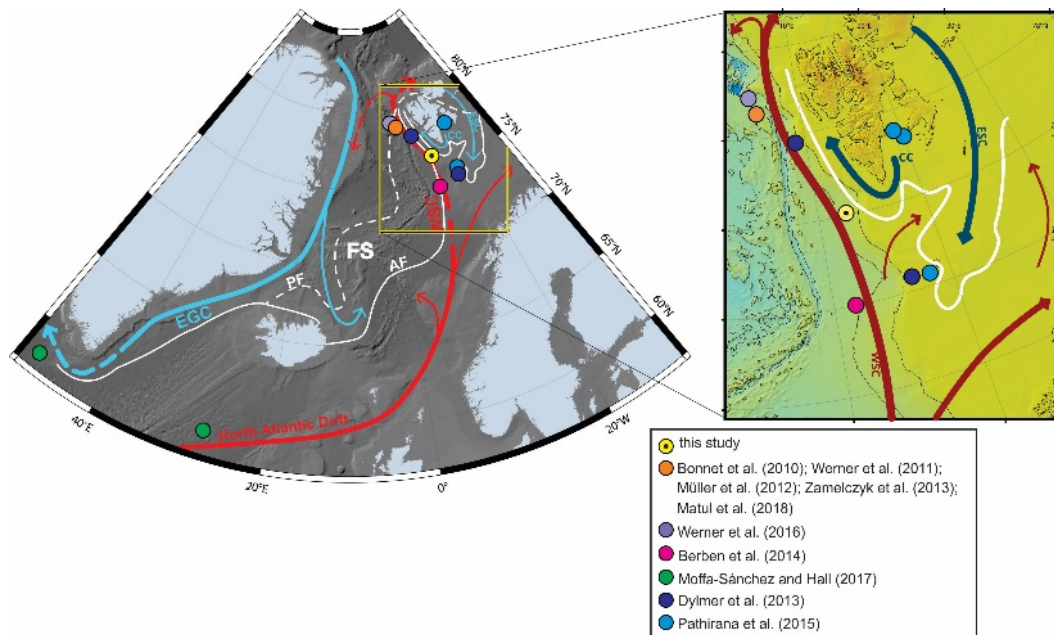
We have shortened the manuscript and re-formulated some parts of the text in a more precise way. We also corrected the English language.

---

The figures and graphs are effective.

But I recommend improving Fig. 1. I would like to see the schematic map of Svalbard margin contains the position of short sediment core (probably some short sediment cores from related papers which will be discussed by authors), and surface circulation pattern, bathymetry. The amount and quality of supplementary material is quite appropriate

We have included a schematic map of the Svalbard margin showing the surface circulation pattern, bathymetry and the position of the sediment cores discussed in the manuscript as recommended by the Reviewer, see below.



## **Anonymous Reviewer #2**

1) The methodology is generally not explained clearly enough, which makes the further interpretation rather unconvincing:

The following sentence (Chapter 2.1, page 5) raises doubts about the good faith of the authors. “The depth-sampling intervals were assigned based on the distribution of water masses recorded by the CTD”. This is simply not true. How can one imagine that there is no change in the vertical water stratification between October and July. Of course there is (see Figure 2)! The 0-50m interval is only correct for the October sampling. In other seasons, the authors sampled a mixture of populations living in the mixed layer and below the thermos/haloclines. The further interpretation based on living faunas is therefore severely compromised.

We acknowledge our mistake in the statement (Chapter 2.1, p. 5, line 16-17) in the submitted version of our manuscript. As Reviewer #2 is pointing out this information is only valid for the October 2012, the time of our core sampling, we have therefore made the necessary changes to the manuscript.

Further, we agree that in other seasons, in 0-50 m water depth we collected a mixture of populations (NB we always collect all populations in these depth-intervals of the water column, never a single population) living in the mixed layer and below the thermo/halocline. As we compare closely to the living planktic foraminifera fauna data from other studies/literature in this region (chapter 3.1.3 Modern distribution and ecology of living high-latitude planktic foraminifera), we think that our interpretation is valid and comparable to other studies. Nevertheless, in order to clarify the issue pointed out by Reviewer #2, we removed the sentence and added the information to Chapter: 3.1.3, new p. 11, lines 6-10:

*“As our plankton tow data are collected in two different years, at two different seasons and different depth intervals (see Methods), we cannot examine possible species-specific living depths. We therefore support our data with published results to establish a record of the*

*modern vertical distribution of planktic foraminiferal species in the surface water column of the study area.”*

---

Planktic foraminiferal (PF) faunas are given in number of specimens per cubic meter (Chapter 2.1, page 5). How was the volume of filtered water measured? The WP2 device cannot be equipped with 2 flowmeters, able to record the “in” and “out” fluxes. Thus to my knowledge, it is difficult to accurately estimate the number of ind/m<sup>3</sup> with a WP2 sampler. A large error margin has to be taken into account, which was not done at all in the paper.

There are two ways to estimate the volume of filtered water: (1) by using a flowmeter and, if a flowmeter cannot be used, (2) by multiplying the net aperture area by depth towed. As the Reviewer #2 correctly points out the WP2 plankton sampler cannot be equipped with a flowmeter, so we use method (2), the calculation to estimate the volume of water that passed through the net (the volume of a cylinder with the length represented by the depth of the tow). In both methods, the accuracy has some errors:

Flowmeters don't work well for vertical tows, because they record the current going down as well and since a perfectly vertical tow recovery is extremely rare (or impossible in moving sea), one have to note the angle the haul line makes with the surface of the water and calculate the hypotenuse to get the true depth.

Method (2) can introduce some uncertainties because mesh-sizes below 200µm can get clogged easily during spring blooms or when gelatinous zooplankton are abundant. As the net becomes progressively clogged as it ascend, it filters less water near the surface than at depth. Also, if one tow up to quickly (faster than 1-2m per second, you may create a pressure wave in front of the rapidly moving net that pushes aside some zooplankton.

During our sampling, we did not record any zooplankton/ algae overabundance and the vertical towing speed was ~ 0.5 m s<sup>-1</sup> (Chapter 2.1, line 17-18) which assured proper and complete recovery of planktic foraminifera (zooplankton).

We have now added how the volume and the number of ind/m<sup>3</sup> were calculated to Chapter 2.1, p. 5, lines 16-19:

*“Vertical towing speed was ~0.5 m s<sup>-1</sup> and the volume of filtered water was measured by multiplying net aperture area by depth towed following the general formula:  $V = \pi r^2 \times L$ , where  $V$  = volume (m<sup>3</sup>) of seawater,  $\pi = 3.1415$ ,  $r^2$  = radius of net opening squared (m<sup>2</sup>),  $L$  = length, distance net was towed (m).”*

---

Chapter 2.2, page 5: what kind of box core was used?

Are the authors sure that the water-sediment interface was properly sampled? If the sampler is not completely closed, a washout may occur when the sampler is being retrieved.

Consequently, to what extent are the PF counts in the surficial sediment correct? Since there is some uncertainty about the quality of this sample, the core top sample should perhaps be discarded.

Technical data of the box core used are: Total height: 2.5 meters; Total length after release is 2.5 meter + 3.3 meter wire = 5.8 meter; The box core is 5-sided where: Shortest wall: 1.95 meter, Longest wall: 2.25 meters; Weight: 1100 kg; Volume of test box: 125 liters; Box dimensions: 50x50x50 cm.

We agree with Reviewer #2 that if the sampler is not completely closed a washout may occur when the sampler is being retrieved. We are well aware of the potential problem, hence in the

rare cases, if the box corer is disturbed, we always consider the sampling as failure and make a new attempt of coring. Furthermore, we are certain that the water-sediment interface was properly sampled in our case. As documentation we include photos of the surface sediment of the boxcore HH12-1206BC after retrieval and removal of seawater (Fig. 1a,b). Moreover, as stated in the manuscript (Results, Chapter 3.2.1, line 13-15) profiles analyzed for activity of  $^{210}\text{Pb}$  and  $^{137}\text{Cs}$  clearly show that 3 cm thick surface layer has the highest and near-uniform activities indicating a surface mixed layer, thereby confirming the recovery of the upper surface sediments of the core.



Figure 1. Two photos of the water-sediment interface in box core HH12-1206BC before pushing the tube into the sediment for subsampling. The disturbance in the lower left corner is from removal of the water with a hose.

---

Chapter 2.2, page 6: A sentence states “The small (100–125µm)- and large (150–180µm)-size shells represent different life stages, the juvenile and adult forms, respectively” I don’t agree with this discrimination of different life stages on this basis of very similar test sizes! The size-fractions proposed here are not appropriate. For example, for *T. quinqueloba*, 125µm diameter is a "normal" adult size. It is a well-known small species... (e.g. Schiebel and Hemleben, 2005; Husum and Hald, 2012).

Given the reported approximate sizes for *T. quinqueloba* in the literature, we agree with Reviewer #2 that the terms “juvenile” and “adult forms” for 100–125µm and 150–180µm, respectively, may be confusing. We therefore removed the sentence and the text now reads, p. 6, lines 26-27:

*“The shells were picked from two narrow size ranges of 100–125 and 150–180 µm.”*

---

Chapter 2.2, page 6: Counting shell fragments is far from trivial. What did the authors count precisely? what sizes of fragments? how to be sure to count only PF fragments?

The characteristic morphology (e.g. porosity, structure) of planktic foraminiferal shells is maintained even after a breakdown of the shell and clearly identifiable in small fragments of planktic foraminiferal shells. The specific structure of the planktic foraminiferal shell is also easily distinguishable from the structure and composition of hyaline and porcellaneous benthic foraminifera and their respective fragments.

We counted small fragments of shell walls in >100 µm size fraction alongside counts and identification of planktic foraminifera.

We included the information on the counted fragments and their size to the chapter 2.2, p. 7, line 1-3:

*“Shell fragments were counted in the >100 µm size fraction alongside counts of planktic foraminifera as an indication for the general preservation state of specimens and species (Berger et al., 1970; 1982).”*

---

2) Some basic interpretations are not correct - Chapter 3.2.2: the authors consider fragmentation as an indicator of bad preservation. Which is correct, but the authors focussed only on CaCO<sub>3</sub> dissolution to explain fragmentation, writing (page 17) “% fragmentation is low indicating well-saturated with respect to calcium carbonate”. Bad preservation can also be due to transport and/or reworking on the sea floor in areas of active bottom currents. Above all, CaCO<sub>3</sub> preservation may be closely linked to early diagenetic processes within the sediment that have nothing to do with the bottom sea characteristics during the deposition!

We completely agree with the comment of Reviewer #2 that changes in preservation can also be due to transport and/or reworking on the sea floor in areas of active bottom currents and, most probably, be closely linked to early diagenetic processes within the sediment. However, we would like to point out that in our multiproxy approach, we only use fragmentation in combination with the shell weight of specimens and the correlation between these two proxies. From Fig. 6, when shell weight is low, % fragmentation is higher and vice versa, which strongly support that the fragmentation in our case is caused by dissolution and not other factors. As our study site is strongly influenced by Atlantic water masses all year round where the sediments are rich in calcium carbonate with high buffering capacity (e.g., Huber et al., 2000), dissolution due to early diagenetic processes seems to be unlikely. We have now

added this to the text to clarify this point in chapter Results, 3.2.2 Planktic foraminifera, mean shell weights and fragmentation, p. 14, line 5-18:

*“The %fragmentation shows an opposite pattern to the mean shell-weight records (Fig. 6a,b), i.e. high %fragmentation corresponds to low shell-weight of planktic foraminifera (Figs. 4f, 6b). As our Storfjorden Fan site is strongly influenced by Atlantic water masses all year round, and located in CaCO<sub>3</sub> rich sediments (Hebbeln et al., 1998), the area has a high buffering capacity of the pore water (Emerson and Bender, 1981; Archer et al., 1989; Huber et al., 2000). The %TOC and %CaCO<sub>3</sub> in core HH12-1206BC are almost constant throughout the record (Fig. 4c,e). Therefore, we can assume that there are no significant changes in preservation of the planktic foraminifera due to diagenetic processes in the recorded time interval and use %fragmentation alongside the mean shell weight records as a proxy for changes in CaCO<sub>3</sub> saturation and influence of Atlantic Water. Furthermore, the core site is located in an area where fine-grained sediment is able to settle out of suspension undisturbed by strong bottom currents (Winkelmann et al., 2005). Thus, potential preservation problems due to transport and/or reworking on the sea floor are negligible.”*

---

Chapter 3.2.4, page 15: “the three CTD casts taken during key-seasons for reproduction of planktic foraminifera at the core site”. What are these key-seasons for PF reproduction at the studied site? The authors suggests that PF reproduction occurs 3 times a year, October, April and July. On which data is this free assumption based? What is the real timing of PF reproduction at the core site? To my knowledge, in this area there is absolutely no information available about PF reproduction seasons.

We agree the Reviewer’s #2 comment on planktic foraminifera reproductive seasons. Now, we see that this sentence “the three CTD casts taken during key-seasons for reproduction of planktic foraminifera at the core site” was poorly formulated. The sentence has been removed, and p. 15, lines 14-16 now reads:

*“These temperatures are very similar to the temperatures (3.9–5.4 °C) recorded at 100–250 m water depth by the three CTD casts (Figs. 21a,b, 8a,c).”*

---

Chapter 3.1.3, page 11: One can read “G. uvula was found at X m water depth..., which could indicate that this depth is the calcification depth of the species”. Unfortunately, the depth of calcification is generally not where you find most individuals! Calcification of PF starts at the reproduction level, possibly close to the pycnocline (for the studied species; Schiebel and Hemleben, 2005), and ends where PF are largest (i.e. end of calcification), just before the reproduction at the same pycnocline level! Calcification depth is still a matter of debate.

We understand Reviewers #2 concern here and we agree that calcification depth of planktic foraminifera is a difficult issue to resolve as it may vary temporally and spatially, in response to environmental conditions, and change during the life-cycle (Rebotim et al., 2017). To avoid confusion we reformulated this part of our manuscript, p. 11, lines 6-10, referring to our reply to the reviewer above concerning point Chapter: 3.1.3, p. 12, lines 6-9.

---

Calcification depths could have been be discussed here with data of the modern fauna (see my point 3).

We reply to this comment below at the Reviewer’s #2 point 3.

---

Chapter 3.1.3 - on page 12 is written: “This species is capable of living in salinities of 30.5–31, which appears to be the minimum salinity for planktic foraminifera (Boltovskoy and Lena, 1970b)”. The authors should have a better look at the available, recent literatures! PF have a high tolerance to salinity changes (e.g., Bijma et al., 1990; Ortiz et al., 1995). They are not directly affected by low salinity (e.g., Fernandez et al., 1991), but rather by parameters that co-vary with salinity (e.g., Ufkes et al., 1998; Retailleau et al, 2009).

We thank the Reviewer #2 for the references and agree with this remark. We have reformulated the sentence to make our point clearer, p. 12, lines 6-9:

“Generally, *G. uvula* lives in the upper 30–50 m of the water column (Boltovskoy et al., 1996, H. Bauch, unpublished data) and is considered tolerant of hyposaline conditions (Boltovskoy and Lena, 1970b; Hemleben et al., 1989).”

---

3) No isotope measurements were performed on the modern living fauna whereas the authors have good material to do this (plankton tows and Rosette CTD). They should have tested all basic interpretations from the literature with their own data set. For example, - compare  $^{18}\text{O}$  and  $^{13}\text{C}$  of the living fauna (trapped in the plankton tows) with measurements of the ambient seawater isotopes. This could help to identify the specific calcification depth. - compare the isotopic differences between living species with the observed water masses and subsequent stratification and thus verify the hypotheses presented on page 3 “*N. pachyderma* and *T. quinqueloba* ( $^{18}\text{ONp-Tq}$ ) as an indicator of the subsurface-to-near surface Atlantic Water relative inflow and between *T. quinqueloba* and *G. uvula* ( $^{18}\text{OTq-Gu}$ ) as an indicator of relative changes in freshening and stratification of the surface waters in the past.”

We could not agree more with Reviewer’s #2 comment, as we had the same idea and have attempted to achieve this. We tried to measure  $\text{d}^{18}\text{O}$  and  $\text{d}^{13}\text{C}$  on *G. uvula* (three times), *N. pachyderma* and *T. quinqueloba* from 0-50, 50-100 and 100-200 m water depth.

Unfortunately, every measurement on *G. uvula* and *N. pachyderma* failed either due to low amount of material or laboratory technical problems. Isotopic measurements on live planktic foraminifera can be challenging, as their shells are thinner and lighter than their paleo counterparts, e.g. a number of 25 of *G. uvula* from the sediment core gave reliable measurements, whereas a number of 80 specimens of live *G. uvula* were not sufficient to detect the isotopic signal and/or produce a reliable result. The only successful measurement according to the laboratory report was made on *T. quinqueloba* from 0-50 m water depth ( $\text{d}^{13}\text{C} = -1.69\text{‰ VPDB}$  and  $\text{d}^{18}\text{O} = 1.84\text{‰ VPDB}$ ).

We did not include nor discuss the two data points in our manuscript as it represents only one sampled depth interval and a comparison to other depths and species was impossible to due to the failed measurements.

We are well aware that isotopic signatures/measurements on modern living fauna alongside other oceanic data (ctd, sea water isotopes) collected simultaneously is of high relevance for the assessments of planktic foraminifera vertical habitats (especially the calcification depth) and crucial for paleoceanography. That’s why we plan this kind of studies with a new strategy sampling of planktic foraminifera in the future.

4) Chapter 1.1 Oceanographic setting, gives in 10 lines a very vague and extremely general view of the studied system (without any reference to literature). It is more than necessary to explain here the seasonal and interannual variability of the intensity and location of the modern AF, on the basis of recent oceanographic measurements.

We have added the requested information to the 1.1 Oceanographic settings chapter, p. 4, lines 9-16:

*“An oceanic front, the Arctic Front (AF) is located where the two water masses meet and is presently located near the core site. The AF is a topographically controlled density barrier (Loeng, 1991). The position of the front depends on the relative strengths in flow of the WSC and the ESC (Vinje, 1977). Sea ice melting during spring and summer often creates a stratified and nutrient-rich euphotic zone, which enhances plankton blooms along the marginal ice zone (e.g., Sakshaug and Slagstad, 1992; Owrid et al., 2000; Pathirana et al., 2014). The marginal ice zone is also determined by the position of the AF (Smith and Sakshaug, 1990).”*

---

5) In chapter 4.2 Sea surface reconstruction: the authors repeat/summarize their results and interpretation for (only) a single 30cm-long core. No clear comparison with other cores sampled in the vicinity (Eastern North Atlantic, west Svalbard) is presented. But a comparison is made with results from the broadly diversified North Atlantic Ocean domain! It would be very surprising if exactly the same processes influence PF faunas in the eastern Labrador area and along western Svalbard! Such comparison, without any reserve, suggests an ignorance of the functioning of the modern oceans. There is no real discussion, with sentences advocating the “success” of their study because it agrees with others! See in chapter 4.2.1 “The warm surface conditions... are in agreement with other studies from the North Atlantic Ocean”; in chapter 4.2.5 “There is a paleoproxy consensus of the progressive warming:” Or the worst, in chapter 4.2.2 “Overall, taking into account differences in sedimentation rates, dating control, and marine reservoir age corrections, a warming: in the Storfjorden Fan can be considered as a widespread phenomenon”

We acknowledge Reviewer #2 comment. We added a new chapter 4.3 Comparison to other studies (page 21-23) where we compare to several other studies based on sediment cores from our region and the North Atlantic. We also shortened and re-formulated some parts of the text and corrected the English language. We partly removed and/or reformulated sentences criticized by Reviewer #2 statements.

Planktic foraminifera and structure of surface water masses at the SW Svalbard margin in relation to climate changes during the last 2000 years

Katarzyna Zamelczyk<sup>1</sup>, Tine L. Rasmussen<sup>1</sup>, Markus Raitzsch<sup>2</sup>, Melissa Chierici<sup>3</sup>

<sup>1</sup> Centre for Arctic Gas Hydrate, Environment and Climate, Department of Geoscience, UiT - The Arctic University of Norway, N-9037 Tromsø, Norway

<sup>2</sup> MARUM - Zentrum für Marine Umweltwissenschaften, Universität Bremen, Leobener Str., 28359 Bremen, Germany

<sup>3</sup> Institute of Marine Research, Box 6404, 9294 Tromsø, Norway

Correspondence to: Katarzyna Zamelczyk (katarzyna.zamelczyk@uit.no)

**Abstract.** We present a high-resolution reconstruction of properties of the subsurface (250–100 m), near surface (100–30 m) and surface (30–0 m) water masses at the SW Svalbard margin in relation to climate change during the last 2000 years. The study is based on the distribution patterns of planktic foraminiferal faunas,  $\delta^{18}\text{O}$  and  $\delta^{13}\text{C}$  values measured on

5 *Neogloboquadrina pachyderma*, *Turborotalita quinqueloba*, and *Globigerinita uvula*, Mg/Ca-,  $\delta^{18}\text{O}$ - and transfer function-based sea surface temperatures, mean shell weights of planktic foraminiferal species and other geochemical and sedimentological data. We also compared paleo-data with modern planktic foraminiferal fauna distributions and the carbonate chemistry of the surface ocean. The results showed that cold sea surface conditions prevailed at ~400–

10 800 AD and ~1400–1950 AD, associated with the local expression of the Dark Ages Cold Period and Little Ice Age, respectively. Warm sea surface conditions occurred at ~21–400 AD, ~800–1400 AD and from ~1950 AD until present and are linked to the second half of the Roman Warm Period, Medieval Warm Period and recent warming, respectively. On the

15 centennial to multi-centennial time scale, sea surface conditions seem to be governed by the inflow of Atlantic water masses (subsurface and near surface) and the presence of sea-ice and the variability of the sea-ice margin (surface water masses). A close correlation of sea surface temperature recorded by planktic foraminifera with total solar irradiance (TSI) changes implies that solar activity could have an influence on the sea surface conditions on the decadal to multi-decadal time scale.

20

## 1 Introduction

The inflow of warm Atlantic Water via the West Spitsbergen Current (WSC) to the Arctic is considered a major controlling factor of climate in the Fram Strait over millennial (e.g., Dokken and Hald, 1996; Rasmussen et al., 2007; Müller et al., 2009; Jessen et al., 2010; Zamelczyk et al., 2012; 2014; Telesinski et al. 2017) to centennial timescales (e.g. Sutton and Hodson, 2005; Majewski et al. 2009; Spielhagen et al., 2011; Zamelczyk et al., 2013; Werner et al., 2016; Pawłowska et al. 2016). Atlantic water masses transported to the Nordic seas converts warm and saline surface water to cold and less saline deep water masses. The heat loss and decrease in salinity depend on the interactions of the surface water with cold melt water and cold air masses (Brambilla et al., 2008). Millennial scale variability in surface ocean circulation and properties of the Atlantic water masses have been documented for the Holocene interglacial period (e.g., Bianchi and McCave, 1999; Oppo et al., 2003; Giraudeau et al., 2010; Van Nieuwenhove et al., 2016) and of past glacial periods (e.g., Hoff et al., 2016). However, apart from a few studies west of Svalbard (Winkelmann et al., 2005; Majewski et al. 2009; Spielhagen et al. 2011; Werner et al., 2011; Zamelczyk et al., 2013; Pawłowska et al. 2016), little is still known about the natural variability of surface and subsurface ocean circulation over the western Svalbard margin on decadal to centennial timescales beyond the last ~200 years. The Roman Warm Period (RWP, ~200 BC–400 AD), the Dark Ages (DA, ~400–800 AD), the Medieval Warm Period (MWP, ~800–1400 AD) and the Little Ice Age (LIA, ~1400–1950 AD (Grove, 2004)) are climate events well-documented in social history of the North Atlantic region (e.g., Lamb 1977). Prior to the anthropogenic changes of the last century, interactions between the warm Atlantic Water and supply of cold polar water were controlled by natural climate anomalies of the past two millennia (e.g., Werner et al., 2011; Zamelczyk et al., 2013; Pathirana et al., 2015; Pawłowska et al. 2016). Freshwater input from melting sea-ice and high frequency physical and chemical changes occurring in the upper surface ocean are relevant for defining and assessing the dynamics of the present ocean and climate changes. These dynamics are an essential part of the deep-water production and hence the Atlantic Ocean's thermohaline circulation (e.g., Rudels, 1995). However, existing Arctic instrumental records are sparse and burdened with great uncertainties with regard to the significance of the recent warming, natural variability and the superimposed anthropogenic influence. Thus, more studies are required for a better

understanding of the timing, spatial extent, local appearance and the magnitude of changes during the past two millennia, particularly in relation to changes in the flow of Atlantic Water.

Planktic foraminifera are a powerful tool to reconstruct sea surface conditions of the past. Individual species of planktic foraminifera preferentially live in specific water masses at and near the sea surface and can be used to assess the properties and variability of the upper water column. The most common planktic foraminiferal species in the modern polar region are *Turborotalita quinqueloba*, *Neogloboquadrina pachyderma* (Carstens et al., 1997; Volkman, 2000), and recently also, *Globigerinita uvula* and its variant *G. uvula minuta* (Hulot, 2015; Meilland et al., 2015; 2016; Schiebel et al., 2017).

The purpose of the present study is to reconstruct the properties of the upper ~250 m of the water column over the southwestern Svalbard margin for the past 2000 years to get a better understanding of the flow of Atlantic Water in relation to climate over historical times on centennial to decadal time scales. The sediment box core HH12-1206BC has been retrieved from Storfjorden Fan southwest of Svalbard in the Atlantic Water influenced part of the Fram Strait. The study is based on the distribution pattern and concentration of planktic foraminifera, and sea surface temperatures (SST) based on Mg/Ca ratios,  $\delta^{18}\text{O}$  values measured on *N. pachyderma* and *T. quinqueloba*, and transfer function-based SST. In addition, we combine the paleo-record with modern planktic foraminifera from plankton tows and the carbonate chemistry of the surface ocean and apply interspecific isotopic relationships and the main, species-specific depth habitats of *G. uvula*, *T. quinqueloba* and *N. pachyderma* to infer oceanic conditions of the surface, near surface and subsurface water masses, respectively. Furthermore, based on the main depth habitats of *N. pachyderma*, *T. quinqueloba* and *G. uvula*, we use the difference in the  $\delta^{18}\text{O}$  values between *N. pachyderma* and *T. quinqueloba* ( $\Delta\delta^{18}\text{O}_{\text{Np-Tq}}$ ) as an indicator of the subsurface-to-near surface Atlantic Water relative inflow and between *T. quinqueloba* and *G. uvula* ( $\Delta\delta^{18}\text{O}_{\text{Tq-Gu}}$ ) as an indicator of relative changes in freshening and stratification of the surface waters in the past. For supporting information, we also use dissolution proxies and other geochemical and sedimentological data. We compare our results from Storfjorden Fan to studies of the Late Holocene from other areas to better assess the nature of large-scale climate forcings.

## 1.1 Oceanographic setting

The near surface oceanographic setting SW off Svalbard Archipelago is characterized by the interaction between temperate and saline Atlantic Water ( $S > 34.92$ ;  $T > 0$  °C) transported by the West Spitsbergen Current (WSC) from south and cooler and less saline Arctic water masses conveyed by the East Spitsbergen Current (ESC) from the east (Fig. 1) (Loeng, 1991).

5 The Coastal Current (CC), which is the extension of the ESC, contains a mixture of Arctic Water and sea-ice transported from the northern Barents Sea and/or produced in Storfjorden. Sea-ice cover in the study area may vary from year to year probably reflecting the inter-annual variability of the Atlantic water inflow (Vinje, 2001).

10 An oceanic front, the Arctic Front (AF) is located where the two water masses meet and is presently located near the core site. The AF is a topographically controlled density barrier (Loeng, 1991). The position of the front depends on the relative strengths in flow of the WSC and the ESC (Vinje, 1977). Sea ice melting during spring and summer often creates a stratified and nutrient-rich euphotic zone, which enhances plankton blooms along the marginal ice zone (e.g., Sakshaug and Slagstad, 1992; Owrid et al., 2000; Pathirana et al., 15 2014). The marginal ice zone is also determined by the position of the AF (Smith and Sakshaug, 1990).

## 20 **2 Material and methods**

### **2.1 Modern oceanographic data and planktic foraminifera**

Temperature and salinity were measured via a SBE Seabird 911 plus CTD (conductivity-temperature-depth) rosette equipped with Niskin bottles aboard the RV Helmer 25 Hanssen at the study site in October 2012, July 2014 and April 2015.

In April 2015, water samples were collected at the study site for surface to subsurface ocean carbonate chemistry (Fig. 2I). The carbonate chemistry was determined using measurements of total dissolved inorganic carbon ( $C_T$ ) and total alkalinity ( $A_T$ ) on samples collected at 200, 100, 50 and 5 m water depth and analyzed at the Institute of Marine 30 Research, Tromsø, Norway.  $C_T$  was determined by using coulometric titration on a VINDTA system and  $A_T$  by using potentiometric titration with weak HCl on a VINDTA system (Marianda, Germany). The analytical methods and sampling for  $C_T$  and  $A_T$  determination have been described in detail in Dickson et al. (2007). In 2015, the precision were  $\pm 1$   $\mu\text{mol kg}^{-1}$  for both  $A_T$  and for  $C_T$ . The accuracy of  $A_T$  and  $C_T$  were determined using Certified

Reference Material (CRM) supplied by A. Dickson (San Diego, USA) by applying a correction factor to the measured values based on the measured CRM value. Values of  $C_T$ ,  $A_T$  and salinity, temperature, and depth for each sample were used as input parameters in a  $CO_2$ -chemical speciation model (CO<sub>2</sub>SYS program) (Pierrot et al., 2006) to calculate the calcium carbonate saturation state ( $\Omega_{Ca}$ ), pH and the carbonate-ion concentration [ $CO_3^{2-}$ ]. The calculations were performed on the total hydrogen ion scale using the hydrogen sulphate [ $HSO_4^-$ ] dissociation constant of Dickson (1990). We used the carbonate system dissolution constants from Mehrbach et al. (1973) refit by Dickson and Millero (1987). The concentration of calcium, [ $Ca^{2+}$ ] is assumed to be proportional to the salinity according to the equation  $10.28 \times S / 35 \mu mol kg^{-1}$  (Mucci, 1983). The thermodynamic solubility products for calcite (K<sub>sp</sub>) are from Mucci (1983).

Living planktic foraminifera were collected immediately after recovering the CTD casts in October 2012 and July 2014 at the coring site using a WP2 (Working Party 2) plankton tow with 90  $\mu m$  mesh-size net and 0.255 m<sup>2</sup> opening. In 2012, vertical depth-sampling intervals were 0–50 and 50–200 m, and in 2014, vertical depth-sampling intervals were 0–50, 50–100 and 100–200 m (Fig. 2II). Vertical towing speed was  $\sim 0.5 m s^{-1}$  and the volume of filtered water was measured by multiplying net aperture area by depth towed following the general formula:  $V = \pi r^2 \times L$ , where  $V =$  volume (m<sup>3</sup>) of seawater,  $\pi = 3.1415$ ,  $r^2 =$  radius of net opening squared (m<sup>2</sup>),  $L =$  length, distance net was towed (m). Immediately after recovery, the samples were sieved over sieves of mesh-sizes 1000  $\mu m$  and 63  $\mu m$ . The size-fraction  $>63 \mu m$  was fixed with 98% ethanol buffered with disodium hydrogen phosphate to prevent dissolution. Additionally, the samples were stained with Rose Bengal (1.0 g l<sup>-1</sup>) in order to discriminate 'live' (shell containing cytoplasm) from 'dead/transported' (no cytoplasm present) individuals (Lutze and Altenbach, 1991). Samples were kept cool until analysis, which was performed in the laboratory at UiT, the Arctic University of Norway, Tromsø. Only live specimens were considered for analysis. The live planktic foraminifera were counted and concentrations calculated as number of specimens per cubic meter (ind. m<sup>-3</sup>).

30

## 2.2 Sediment core

Box core HH12-1206BC (76°24' N; 012°58' E) was retrieved from Storfjorden Fan from 1520 m water depth during a cruise with RV *Helmer Hanssen* to the Fram Strait in October 2012 (Fig. 1). A tube of inner diameter 10 cm was pushed into the sediment for subsampling. The 30.5 cm long sediment core was sampled at 0.5 cm intervals in the laboratory at UiT, the Arctic University of Norway, Tromsø. Subsequently, the samples were weighed, freeze-dried, weighed again, and the water content (%) was calculated. The dry samples were wet sieved through mesh-sizes 1 mm, 500 µm, 100 µm, and 63 µm following the preparation methods of Feyling-Hanssen et al. (1971) and Knudsen (1998). The residues were dried at room temperature and weighed.

The grain size distribution was calculated as the weight percentage of the residue relative to total dry weight of the sample. The ice-rafted debris (IRD) was counted in the >500 and >150 µm size-fractions. The 150 µm size-fraction was obtained by dry-sieving of the 100–500 µm fraction after counts and identification of foraminifera.

Total carbon (TC) and total organic carbon (TOC) were measured in bulk samples using a Leco CS-200 induction furnace instrument. The weight percentage (wt %) of TC and TOC was calculated in intervals of 1–2 cm. The CaCO<sub>3</sub> content (wt %) was calculated using the following equation:  $\text{CaCO}_3 = (\text{TC} - \text{TOC}) \times 8.33$  (Espitalié et al., 1977).

The fraction 100–500 µm was split and a representative number of planktic foraminifera specimens (>300) were picked from the >100 µm size fraction, counted and identified to species level. The number of foraminifera per gram dry weight sediment was calculated.

Relative changes in mean foraminiferal shell weight can be interpreted as changes in shell thickness, changes in preservation and the extent of calcification (Lohmann, 1995; Barker and Elderfield, 2002; Barker et al., 2004; Zamelczyk et al., 2012, 2013). The shells of the planktic foraminiferal species *N. pachyderma* and *T. quinqueloba* were weighed using a Sartorius microbalance (model M2P, 0.1 µg sensitivity). The shells were picked from two narrow size ranges of 100–125 and 150–180 µm. Mean shell weights were calculated by dividing the weighed total mass of 20–30 individuals in each size range by the number of weighed shells. Due to low abundances of *T. quinqueloba*, 16 samples from the 100–125 µm size-fraction and 15 samples from the 150–180 µm size-fraction contained less than 10 individuals. All measurements were repeated 3 times. Shells with sediment fill or showing signs of mechanical corrosion at the outer shell surface or having visually detectable secondary calcite crust were omitted.

Shell fragments were counted in the >100  $\mu\text{m}$  size fraction alongside counts of planktic foraminifera as an indication for the general preservation state of specimens and species (Berger et al., 1970; 1982). The number of fragments per gram dry weight sediment was calculated and the percent fragmentation was calculated relative to the total numbers of planktic foraminifera  $\text{g}^{-1}$  and the total number of fragments  $\text{g}^{-1}$  in a sample.

Stable isotopes were measured on the three species *N. pachyderma*, *T. quinqueloba* and *G. uvula minuta* from size-fractions 125–150  $\mu\text{m}$ , 150–180  $\mu\text{m}$  and 100–150  $\mu\text{m}$ , respectively. The measurements were done at the Leibniz Laboratory for Radiometric Dating and Stable Isotope Research in Kiel, Germany, using an automated Carbo-Kiel device connected to a Finnigan MAT 253 and MAT 252 mass spectrometers. Results refer to the Vienna Pee Dee Belemnite (VPDB) standard. The external analytical reproducibility was <0.06‰ and <0.03‰ for  $\delta^{18}\text{O}$  and  $\delta^{13}\text{C}$ , respectively. Measurements on all three species were carried out at 0.5 to 2 cm intervals. Between 7 and 10 cm core depth, absence of *T. quinqueloba* and *G. uvula* specimens prevented analysis.

The first top 12 samples (upper 6.5 cm) were analyzed for activity profiles of  $^{210}\text{Pb}$  and  $^{137}\text{Cs}$  in order to determine the modern sedimentation rate, assess the recovery of core top sediments and to establish the age of the youngest sediments. Freeze-dried and homogenized samples were analyzed using a high-resolution germanium diode gamma detector and multichannel analyzer gamma counter at the Centre d'Études Nordiques (CEN), Université Laval (Canada). Prior to analysis, the samples were put into plastic vials to rest for at least three weeks to attain the secular equilibrium. The linear apparent sedimentation rate was calculated from the decrease of excess  $^{210}\text{Pb}$  activities with sediment depth following McKee et al. (1983). Excess  $^{210}\text{Pb}$  activities were determined by subtracting the average supported activity (average of  $^{214}\text{Pb}$ ,  $^{214}\text{Bi}$  and  $^{226}\text{Ra}$ ) from the total activity (Fig. 3a). The  $^{210}\text{Pb}$ -derived sedimentation rate was confirmed using the first occurrence of  $^{137}\text{Cs}$  as a marker of the early 1950s (Robbins and Edgington, 1975).

Nine accelerator mass spectrometry (AMS)  $^{14}\text{C}$  ages were achieved on monospecific samples of *N. pachyderma*, except ages at 4.5–6.5 and 13–14 cm, where all available planktic foraminifera were picked. Measurements were performed at the Poznań Radiocarbon Laboratory, Poland (Table 1). The dates were calibrated into calendar ages using the calibration program CALIB Rev. 7.0.2 (Stuiver & Reimer, 1993) and the Marine13 calibration data set (Reimer et al., 2013). A global average marine reservoir age of 400 radiocarbon years and  $7\pm 11$   $^{14}\text{C}$  years of local deviation ( $\Delta\text{R}$ ) (Mangerud et al., 2006) was

applied. The sample from 2.0–3.5 cm core depth most likely contained modern, post-A-bomb carbon, indicating a post-1950 age. Samples at 4.5–6.5 cm and at 9.5–11.5 cm gave inverted ages probably due to mixing of sediment either representing re-deposition events or a possible error introduced by the very small amount of material (0.01–0.02 mgC) used (Table 1). These three dates were not used in the construction of the age model. The calibrated ages are reported as years AD with a  $2\sigma$  standard error.

**Elemental ratios** of Mg/Ca and Al/Ca were measured on *N. pachyderma* (60–130 shells/sample) at 0.5 to 2 cm resolution. Clean, well-preserved shells with no visible signs of dissolution were picked from a narrow size fraction of 150–180  $\mu\text{m}$ . Prior to analysis, the foraminiferal shells were crushed and cleaned in the clean-lab at the Alfred Wegener Institute (AWI), Bremerhaven, Germany. The cleaning procedure principally followed the protocol given in Barker et al. (2003). The procedure included four steps: clay removal with boron-free MQ water and methanol, oxidation of organic matter in NaOH-buffered  $\text{H}_2\text{O}_2$ , weak acid leach in 0.001 N HCl, and carbonate dissolution in 0.2 N HCl. Subsequently, from each sample an aliquot of 5  $\mu\text{L}$  was diluted with 2%  $\text{HNO}_3$  to determine the Ca concentration. Finally, the remaining residue was diluted with 2%  $\text{HNO}_3$  to obtain a Ca concentration of 15 to 20 ppm. The samples were analyzed using a Nu AttoM high resolution double-focusing inductively coupled plasma mass spectrometer at AWI, Bremerhaven. Five replicates were carried out for every sample. Long-term precision ( $2\sigma$ ) of analyses for Mg/Ca is 2.8%. Since sample material was very limited, analyses were conducted at a Ca concentration of  $\sim 15$  ppm. The measurement uncertainty was determined by analyzing the carbonate standard JcT-1 (giant clam) yielding Mg/Ca ratios of  $1.28 \pm 0.05$  ( $\pm 2\sigma$ ) mmol/mol, which is within 1% of the values reported in the literature (Inoue et al., 2004; Hathorne et al., 2013).

Al/Ca ratios in the foraminiferal samples were used to detect potential clay contamination that might bias the Mg/Ca ratios measured in the foraminiferal calcite (Rosenthal et al., 2000; Barker et al., 2003). No significant correlation between Al/Ca and Mg/Ca ( $R^2 = 0.15$ ) was found. Three samples with Al/Ca  $> 0.80$  mmol/mol (Barker et al., 2003) were omitted. No correlation between high Al/Ca ratios and outliers within the Mg/Ca data set was present. We conclude that the measured high Al/Ca ratios did not affect the Mg/Ca signal. In the results and discussion sections, we will discuss the Mg/Ca-based temperature profiles instead of the Mg/Ca ratios since both are exactly the same and the temperature reconstructions allow us to compare with other temperature reconstructions in our study.

### 2.2.1 SST calculations based on $\delta^{18}\text{O}$ , Mg/Ca ratios and transfer functions

Reconstructions of sea surface temperatures (SST) were calculated based on measured  
5  $\delta^{18}\text{O}$ , Mg/Ca ratios and transfer functions. The average calcification temperature were  
calculated from measured  $\delta^{18}\text{O}$  values ( $\text{SST}_{\delta^{18}\text{O}}$ ) using the equation of Shackleton (1974):

$$\text{(Eq.1) } T (\text{°C}) = 16.9 - 4 * (\delta^{18}\text{O}_{\text{foram, vs. V-PDB}} + \delta^{18}\text{O}_{\text{vital effect, vs. V-PDB}} - \delta^{18}\text{O}_{\text{water, vs. V-SMOW}}),$$

10

where  $\delta^{18}\text{O}_{\text{water}}$  is standard mean ocean water composition (V-SMOW). Conversion from the  
Standard Mean Ocean Water (SMOW) scale to calcite on the Pee Dee Belemnite (PDB) scale  
was done by subtracting 0.2‰ (Shackleton, 1974). For tentative temperature calculations, a  
constant value of 0.3‰ PDB for paleo- $\delta^{18}\text{O}_{\text{water}}$  was used. This value is considered as the  
15 average modern value on the West Spitsbergen margin at 25–500 m water depth (Meredith et  
al., 2001). A vital effect correction of 0 and +0.7‰ was applied for *N. pachyderma* and *T.*  
*quinqueloba*, respectively (Jonkers et al., 2010).  $\text{SST}_{\delta^{18}\text{O}}$  are calculated assuming a constant  
salinity of 35.1.

The measured Mg/Ca ratios were used to calculate temperatures ( $\text{SST}_{\text{Mg/Ca}}$ ) by using  
20 the species-specific (*N. pachyderma*) linear equation of Kozdon et al. (2009):

$$\text{(Eq. 2) } \text{Mg/Ca (mmol/mol)} = 0.13 * T + 0.35$$

This calibration is based on core-top samples of *N. pachyderma* from the Nordic Seas and  
25 produces reliable  $\text{SST}_{\text{Mg/Ca}}$  estimates at temperatures above ~3 °C (Kozdon et al., 2009).

Transfer functions were used to reconstruct SST based on the census data of the  
planktic foraminiferal species distribution. The statistical method is built on a comparison  
between modern oceanographic data (summer SST at 10 m depth) and compositions of the  
planktic foraminiferal faunas in the >100  $\mu\text{m}$  size-fraction from surface sediments collected in  
30 the Arctic areas influenced by Atlantic Water in the Nordic Seas (Husum and Hald, 2012).  
The data were processed using the data analysis program C2 version 1.3 (Juggins, 2010).  
Several statistical methods were tested. The most precise estimate assessed by the root mean  
squared error of prediction (RMSEP) is indicative for the most predictive transfer function

model, but it may also carry a possible spatial auto-correlation bias in the training set causing overoptimistic estimates of the RMSEP (Telford and Birks, 2005). This bias is most reduced for the Maximum Likelihood (ML) model (Telford and Birks, 2005). The ML-based SST reconstruction is therefore considered as the best representative model for the present record. Moreover, ML-calculated SSTs are close to modern water temperature ranges of the core site and follow the actual fluctuations in species composition of the planktic foraminiferal faunas.

### 3 Results

#### 3.1 Modern data

##### 3.1.1 Temperature and salinity

The CTD casts identified a ~50 m thick, mixed layer of melt water characterized by low salinity (except October 2012) and relatively high temperatures ( $T \sim 6.3^\circ\text{C}$  in October,  $7.9\text{--}5.4^\circ\text{C}$  in July and  $4.1\text{--}4.7^\circ\text{C}$  in April) (Fig. 2Ia,b). From ~50 m to 500–600 m water depth a thick layer of warm and saline Atlantic Water is defined by temperatures ranging from  $1.5^\circ\text{C}$  to  $6.3^\circ\text{C}$  in October 2012,  $0.6^\circ\text{C}$  to  $5.4^\circ\text{C}$  in July 2014, and from  $2.2^\circ\text{C}$  to  $4.7^\circ\text{C}$  in April 2015 (Fig. 2Ia,b). The Atlantic water masses overlie the cold intermediate waters ( $T < 0^\circ\text{C}$ ) generated by convection in the Nordic Seas (e.g., Blindheim et al., 2000). In summer and autumn, the coring site is ice-free, whereas in spring and winter the sea-ice incursion depends on the intensity of drift ice carried by the ESC and the production of sea-ice in Storfjorden (NSIDC).

##### 3.1.2 Carbonate chemistry of the study area

The  $\Omega_{\text{Ca}}$  value is expressed by the product of concentrations of calcium ions [ $\text{Ca}^{2+}$ ] and [ $\text{CO}_3^{2-}$ ] in sea water divided by the solubility product ( $K_{\text{sp}}$ ) at a given temperature, salinity and pressure. When  $\Omega > 1$ ,  $\text{CaCO}_3$  will be kept in solid state and when  $\Omega < 1$ ,  $\text{CaCO}_3$  will tend to dissolve. In April 2015, the surface and subsurface waters (upper 200 m) were well saturated with respect to calcite ( $\Omega_{\text{Ca}}$  ranges from 2.8 at the surface to 2.66 near 200 m

water depth, Fig. 2Ic). Both the carbonate ion concentration  $[\text{CO}_3^{2-}]$  and the concentration of  $\text{CO}_2$  (shown as pH), showed a decrease from the surface to 200 m water depth (Fig. 2Ic).

### 3.1.3 Modern distribution and ecology of living high-latitude planktic foraminifera

5

As our plankton tow data are collected in two different years, at two different seasons and different depth intervals (see Methods), we cannot examine possible species-specific living depths. We therefore support our data with published results to establish a record of the modern vertical distribution of planktic foraminiferal species in the surface water column of the study area.

10

Maximum absolute abundances of *T. quinqueloba* are found in July 2014 at 0–100 m water depth (Fig. 2II). *Turborotalita quinqueloba* is generally considered a photic-zone species due to its symbionts and food requirements (Hemleben et al., 1989). In open and ice-free waters of the Fram Strait, the photic zone and the calcification depth of *T. quinqueloba* can reach ~200 m water depth (Carstens et al. 1997). However, during spring/summer stratification, peaks in primary production absorb and reflect most of the sunlight limiting the depth of the photic zone and cause upward migration of the species (Hemleben et al., 1989). In the Fram Strait, Simstich et al. (2003) and Sarnthein and Werner (2017) report a calcification depth of *T. quinqueloba* not deeper than 30–70 m.

15

20

In both seasons, *N. pachyderma* showed a maximum in absolute abundances in the deeper layers, where Atlantic water masses occupy the water column throughout the year (150–200 m water depth in July 2014), Fig. 2Ia,b). Generally, this species has been classified as a deep-dwelling species, which calcifies around 200 m water depth (Volkman et al., 2001; Simstich et al., 2003; Sarnthein and Werner, 2017). However, the depth of maximum abundance varies from region to region suggesting that their abundance and shell chemistry are tied to density horizons or other conditions (such as food availability) (e.g., Volkman et al., 2001; Simstich et al., 2003; Sarnthein and Werner, 2017). In the Fram Strait, the average depth of calcification of *N. pachyderma* lies between 100 and 200 m water depth (Bauch et al., 1997). The depth may vary depending on the water mass distribution and sea-ice cover (e.g., Volkman et al., 2001). *Neogloboquadrina pachyderma* seems to descend down to 250 m water depth in the Atlantic Water off Norway (Simstich et al., 2003) and below 200 m water depth in the subsurface Atlantic water in the eastern Fram Strait (e.g., Volkman et al., 2001; Pados and Spielhagen, 2014; Pados, et al., 2015).

25

30

*Globigerinita uvula* was found at 0–50 m and at 100–200 m water depth only in July 2014 (Fig. 2II), which could indicate a wide living depth range of this species (Fig. 2II). However, its presence in the upper 50 m suggest that the mixed uppermost layer of the ocean is the preferred habitat for this species during some part of its life cycle. This assumption would be consistent with the average living depth of *G. uvula minuta* in the subtropical North Atlantic, where it is found at  $15 \pm 9$  m water depth (Rebotim et al., 2017). Generally, *G. uvula* lives in the upper 30–50 m of the water column (Boltovskoy et al., 1996, H. Bauch, unpublished data) and is considered tolerant of hyposaline conditions (Boltovskoy and Lena, 1970b; Hemleben et al., 1989).

10

### 3.2 Paleo-data from sediment core HH12-1206BC

#### 3.2.1 Age model, sedimentation rate and sedimentology

15

The  $^{210}\text{Pb}$  and  $^{137}\text{Cs}$  activity profiles show a typical decrease with depth to 6.25 cm. The 3 cm thick surface layer has the highest and near-uniform activities indicating mixing and presence of the upper surface mixed layer and recovery of the actual sediment surface. From 3.25 cm,  $^{210}\text{Pb}$  activities decrease exponentially down to 6.25 cm of the core. The average apparent sedimentation rate is  $0.08 \text{ cm yr}^{-1}$  with a maximum of  $0.1 \text{ cm yr}^{-1}$  (Fig. 3a). Marine sediments of the north Atlantic and the Barents Sea of the past ~100 years may be described by three major peaks in the  $^{137}\text{Cs}$  activity profiles, which are related to the initial atmospheric nuclear bomb testing centered in the fifties to sixties and in the mid-seventies, and the Chernobyl reactor accident in 1986 (Kunzendorf and Larsen, 2002). The  $^{137}\text{Cs}$  activity in the HH12-1206 BC core does not reveal any evident  $^{137}\text{Cs}$  peaks also indicating mixing of the upper 3-cm layer (Fig. 3a). Including the ~3 cm thick surface mixed layer the average sedimentation rate based on  $^{137}\text{Cs}$  activity becomes  $0.07 \text{ cm yr}^{-1}$  (Fig. 3a), which is close to the  $^{210}\text{Pb}$ -derived value. These rates are similar to sedimentation rate reported for the Barents Sea which range from  $0.06\text{--}0.09 \text{ cm yr}^{-1}$  to  $0.10\text{--}0.14 \text{ cm yr}^{-1}$  dependent on whether the upper mixed layer is included in the calculations or not, respectively (Maiti et al., 2010; Vare et al., 2010; Pathirana et al., 2014; 2015 and references therein).

25  
30

The age model was further constrained using six of nine AMS  $^{14}\text{C}$  ages (Table 1, Fig. 3b). A constant sedimentation rate between the dated levels was assumed. The age model

indicates that the core covers the time period from ~21 to ~2012 AD (Fig. 3b). The mean sedimentation rate is ~16 cm kyr<sup>-1</sup>. Between ~1420 and ~1060 AD, sedimentation rate is lowest ~6 cm kyr<sup>-1</sup>, and in the upper part (~1960 AD to present), the sedimentation rate is highest reaching ~53 cm kyr<sup>-1</sup>. This value is considered to be close to the value of sedimentation rate estimated by the <sup>210</sup>Pb (80 cm kyr<sup>-1</sup>) and <sup>137</sup>Cs (70 cm kyr<sup>-1</sup>) activity profiles. Due to reversed <sup>14</sup>C dates within the interval 6.5– ~11.5 cm, the time period from ~1800–~1950 AD is considered to contain potential re-deposition events and is therefore interpreted with great caution.

The sediment is dominated by clay and silt (61–96%) with generally low sand content but a small increase toward the core top (Fig. 4b). The concentration of IRD >1 mm and 500–1000 μm is generally low, however, from ~1750 AD to present, the IRD 500–1000 μm increase towards the top (Fig. 4a).

### 3.2.2 Planktic foraminifera, mean shell weights and fragmentation

Generally, the planktic foraminiferal assemblages in core HH12-1206BC are dominated by *N. pachyderma* (33–88%) except for the core top where *T. quinqueloba* dominates (9–43%) (Fig. 4g,h). The third most abundant species is *Globigerinita uvula*/*G. uvula minuta* (2–20%) that, until recently, has been rarely recorded in the Arctic region (Fig. 4i). However, studies of plankton tows collected in 2014 at the western western Barents Sea margin have shown that *G. uvula* constituted 25 to 64% of the planktic foraminiferal assemblages (Hulot et al., 2015). The increasing relative abundances of this species in the living planktic foraminiferal fauna in the Fram Strait (Schiebel et al., 2017) may indicate the beginning of the long-lasting change of species composition due to changing hydrographic conditions in the Fram Strait (Walczowski et al., 2017). Therefore, we include visual documentation and a short presentation of the species. *Globigerinita uvula minuta* is morphologically similar to *G. uvula*, but has larger, more strongly inflated chambers (Fig. 5). *Globigerinita uvula minuta* is associated with warmer waters than *G. uvula* (Parker 1962; Rögl and Bolli, 1973), while *G. uvula* is indicative for relatively cold nutrient-rich waters and the productive zones of the oceanic fronts (Saito et al., 1981; Boltovskoy et al., 1996; Bergami et al., 2009). Both forms, *G. uvula* and *G. uvula minuta* were found in the Storfjorden Fan record, but not separated. Therefore, we refer to both forms as *G. uvula*.

Other species present in the record are *N. incompta*, *G. glutinata*, and *Globigerina bulloides* (the two latter are not included in the figure as they were always <1%).

Mean shell-weights of both size fractions 100–125 and 150–180  $\mu\text{m}$  of *N. pachyderma* and *T. quinqueloba* show relatively low variability (Fig. 6a). The shell weights indicate a similar response to environmental changes and/or dissolution of the two species (Fig. 6a). The % fragmentation shows an opposite pattern to the mean shell-weight records (Fig. 6a,b), i.e. high % fragmentation corresponds to low shell-weight of planktic foraminifera (Figs. 4f, 6b). As our Storfjorden Fan site is strongly influenced by Atlantic water masses all year round, and located in  $\text{CaCO}_3$  rich sediments (Hebbeln et al., 1998), the area has a high buffering capacity of the pore water (Emerson and Bender, 1981; Archer et al., 1989; Huber et al., 2000). The %TOC and % $\text{CaCO}_3$  in core HH12-1206BC are almost constant throughout the record (Fig. 4c,e). Therefore, we can assume that there are no significant changes in preservation of the planktic foraminifera due to diagenetic processes in the recorded time interval and use % fragmentation alongside the mean shell weight records as a proxy for changes in  $\text{CaCO}_3$  saturation and influence of Atlantic Water. Furthermore, the core site is located in an area where fine-grained sediment is able to settle out of suspension undisturbed by strong bottom currents (Winkelmann et al., 2005). Thus, potential preservation problems due to transport and/or reworking on the sea floor are negligible.

### 3.2.3 Stable isotopes

The  $\delta^{18}\text{O}$  values of *N. pachyderma* and *T. quinqueloba* generally show an increasing trend with lower  $\delta^{18}\text{O}$  values from ~1800 AD (Fig. 7Ia,b). The record of *T. quinqueloba* is more variable than the record of *N. pachyderma*. The  $\delta^{18}\text{O}$  values of *G. uvula* show the opposite trend of the other two species, but of lower amplitude (Fig. 7Ic).

The  $\delta^{13}\text{C}$  values of *N. pachyderma*, *T. quinqueloba* and *G. uvula* show similar trends until ~1800 AD, where the records of *N. pachyderma* and *T. quinqueloba* become highly variable and with high magnitude changes in *T. quinqueloba* (Fig. 7Id–f). The  $\delta^{13}\text{C}$  values of *G. uvula* are low between ~400 AD and ~1760 AD and otherwise high.

The  $\delta^{18}\text{O}$  and  $\delta^{13}\text{C}$  values of *N. pachyderma*, *T. quinqueloba* and *G. uvula* reveal three distinct clusters (Fig. 7II). *Globigerinita uvula* shows lowest  $\delta^{18}\text{O}$  values (0.30–1.48‰) and lowest  $\delta^{13}\text{C}$  values (-2.45– -0.96‰), while *N. pachyderma* have highest  $\delta^{18}\text{O}$  values (2.77–3.35‰) and highest  $\delta^{13}\text{C}$  values (-0.03–0.23‰). The values of *T. quinqueloba* are

intermediate with  $\delta^{18}\text{O}$  values 2.28–2.69‰ and  $\delta^{13}\text{C}$  -1.35– -0.64‰. The offset between average values of  $\delta^{18}\text{O}_{\text{Np}} - \delta^{18}\text{O}_{\text{Tq}}$  is 0.6‰,  $\delta^{18}\text{O}_{\text{Tq}} - \delta^{18}\text{O}_{\text{Gu}}$ , 1.39‰ and  $\delta^{13}\text{C}_{\text{Np}} - \delta^{13}\text{C}_{\text{Tq}}$  is -2.48‰, and  $\delta^{13}\text{C}_{\text{Tq}} - \delta^{13}\text{C}_{\text{Gu}}$ , 0.68‰.

### 5 3.2.4 SST

As presented above (Sect. 3.1.3.), the modern main depth habitats of the studied three species, can be defined as follows: surface 0–~30 m is the living depth range for *G. uvula*, near surface ~30–100 m is the living depth range for *T. quinqueloba*, and subsurface ~100–250 m is the living depth range for *N. pachyderma*. Thus, the SST estimates ( $\text{SST}_{\text{Mg/Ca}}$  and  $\text{SST}-\delta^{18}\text{O}_{\text{Np}}$ ) and other proxies based on *N. pachyderma* refer to subsurface water masses, the  $\text{SST}-\delta^{18}\text{O}_{\text{Tq}}$  based on *T. quinqueloba* refer to temperatures of the near surface, and the  $\text{SST}_{\text{TF}}$  estimated for 10 m water depth is associated with the surface water masses.

Temperatures based on Mg/Ca ratios ( $\text{SST}_{\text{Mg/Ca}}$ ) and  $\delta^{18}\text{O}$  (both *T. quinqueloba* and *N. pachyderma*) vary between 3.1 and 6.2 °C, and 3.4 and 6.6 °C, respectively (Fig. 8a,b). These temperatures are very similar to the temperatures (3.9–5.4 °C) recorded at 100–250 m water depth by the three CTD casts (Figs. 2Ia,b, 8a,c). Comparison of the SST reconstructed from  $\delta^{18}\text{O}_{\text{Np}}$  and  $\delta^{18}\text{O}_{\text{Tq}}$  show an average difference of 1.3 °C (0.3–2.6 °C). SST based on  $\delta^{18}\text{O}$  *T. quinqueloba* clearly show lower temperatures throughout the entire record. The  $\text{SST}-\delta^{18}\text{O}_{\text{Np}}$  vary between 4.7 and 6.6 °C and the  $\text{SST}-\delta^{18}\text{O}_{\text{Tq}}$  show more variable temperatures oscillating between 3.4 and 5.5 °C (Fig. 8a,b). The sea surface temperatures obtained by transfer functions ( $\text{SST}_{\text{TF}}$ ) ranges between 2.0 and 7.0 °C (Fig. 8c). Highest temperatures in the record are noted for the last century.

## 25 4 Discussion

### 4.1 Validation and suitability of the stable isotope SST-reconstructions on *N. pachyderma*, *T. quinqueloba* and *G. uvula*

30 As foraminifera precipitate their calcite from the surrounding seawater it is expected that the  $\delta^{18}\text{O}$  values record the isotopic equilibrium of the seawater and the temperature at the calcification depth of a particular species (Emiliani, 1954). However, due to the differential isotopic uptake in calcareous organisms compared to equilibrium conditions, an offset

between the  $\delta^{18}\text{O}$  values of equilibrium calcite and the measured values of the foraminiferal shells is found (Erez, 1978). This offset (the “vital effect”) is species-specific and varies strongly regionally (Ezard et al., 2015 and references herein). Given the discrepancy and different magnitudes of vital effects reported in the Fram Strait of both  $\delta^{18}\text{O}$  and  $\delta^{13}\text{C}$  of *N. pachyderma* and *T. quinqueloba* (Table 2), and to our knowledge yet non-existing isotope data performed on *G. uvula*, we do not apply any correction for vital effects. We prefer to interpret the oxygen and carbon isotope records addressing general trends rather than absolute numbers. In addition, we validate the suitability of the  $\delta^{18}\text{O}$  and  $\delta^{13}\text{C}$  records by briefly discussing other potential main effects influencing the carbon and oxygen isotopes signatures recorded in shells of the three species studied here.

Planktic foraminiferal interspecific isotopic relationships reflect the isotopic structure of the water column. Shallow dwelling species typically have relatively low  $\delta^{18}\text{O}$  values, compared to deeper dwelling species (Ravelo and Fairbanks, 1992, 1995; Coxall et al., 2007; Birch et al., 2013). In our record, the increase in  $\delta^{18}\text{O}$  values from the surface species *G. uvula*, through near surface dwelling *T. quinqueloba* to subsurface living *N. pachyderma* is well documented and can simply be ascribed to the salinity increase and temperature decrease with depth (lowest values at the surface) (Fig. 7Ia–c). The  $\delta^{13}\text{C}$  values are expected to decrease from surface to subsurface dwelling species, because high primary production and photosynthesis remove the  $^{12}\text{C}$  and enriches the surface water masses in  $^{13}\text{C}$  (Fogel and Cifuentes, 1993). The  $\delta^{13}\text{C}$  of *G. uvula*, as a shallow dweller, should have been high (enriched in  $^{13}\text{C}$ ) compared to *T. quinqueloba* and *N. pachyderma*. However, our records show the opposite (Fig. 7Id–f). The  $^{13}\text{C}$  is a function of dissolved inorganic carbon in the water (Duplessy, 1978) that can be influenced by an array of physical, chemical and biological factors (e.g., Spero et al., 1997; Bemis et al., 2000; Peeters et al., 2002; Chierchi and Fransson, 2009). It is therefore very difficult to explain these inverted values in the highly variable environmental conditions of the Fram Strait. In the case of *T. quinqueloba* and *N. pachyderma* these variable  $\delta^{13}\text{C}$  values could also be associated with the species- and depth-specific isotopic uptake compared to equilibrium conditions (Table 2).

#### 4.2 Interpretation of sea surface conditions over Storfjorden Fan, and climatic inferences

There is at present no consensus on the precise dating, spatial extent, local occurrence and the magnitude of climatic changes that occurred in the last two millennia in the Northern Hemisphere (IPCC, 2014). Therefore, we discuss the data on the basis of major changes in the proxy records, which correlate closely in time with climatic and historical periods defined in Europe by Lamb (1977) (Figs.4, 6–8). In addition, small/large differences in  $\Delta\delta^{18}\text{O}_{\text{Np-Tq}}$  are interpreted as an indication of relative increased/decreased influence of warm and salty Atlantic Waters in the subsurface to near surface water masses and the  $\Delta\delta^{18}\text{O}_{\text{Tq-Gu}}$  as an indication of increased/decreased freshening, i.e. relative presence of melt water/polar water and a measure of strength of stratification of the surface water column. We apply the relative abundance of *G. uvula* as an independent indicator of relatively low salinity surface waters (Hemleben et al., 1989; Boltovskoy and Lena, 1970b) (Fig. 8d–f).

#### 4.2.1 ~21 – ~400 AD, the second half of the Roman Warm Period, RWP

High relative abundance of the subpolar species *T. quinqueloba*, which is indicative of warm and saline Atlantic water inflow (Volkman, 2000), together with high concentration of planktic foraminifera suggest favourable conditions at the sea surface (Fig. 4f,h). The mean shell weights are high and the %fragmentation is low indicating the Atlantic water masses were well-saturated with respect to calcium carbonate (e.g., Huber et al., 2000), except for a short-lasting interval at ~140 AD, when the %fragmentation increased (Fig. 6). The mean shell weight of *N. pachyderma* (150–180  $\mu\text{g}$ ) reaches a maximum of 3.32  $\mu\text{g}$  around ~300 AD indicating strong influence of Atlantic Water. Generally, high mean shell weights of all species, low %TOC, and other parameters indicate overall very good preservation (Figs. 4c,e, 6a,g), similar to a record from northwest Svalbard ~317 km north of the Storfjorden Fan core site at 0–200 AD (Zamelczyk et al., 2013). Preservation patterns at both these sites point to a strong influence of calcium carbonate-rich Atlantic water masses in the eastern Fram Strait during the second half of the Roman Warm Period.

All SST estimates unanimously indicate presence of warm and saline water masses (Fig. 8a–c). The  $\delta^{18}\text{O}$  values of *N. pachyderma* and *T. quinqueloba* are low but relatively high in *G. uvula* possibly indicating stratification of the surface water masses. At ~200–350 AD, maximum SST is recorded, suggesting the influence of Atlantic water masses to be strongest (Fig. 8a–c). Also, the elevated  $\Delta\delta^{18}\text{O}_{\text{Np-Tq}}$  indicate increased subsurface and near surface inflow of Atlantic Water (Fig. 8d). At the same time, the  $\Delta\delta^{18}\text{O}_{\text{Tq-Gu}}$  and the %*G. uvula* are

high, also pointing to increased stratification (Fig. 8e,f). Moreover, the  $\delta^{13}\text{C}_{\text{Gu}}$  values indicate productive surface water, whereas the  $\delta^{13}\text{C}_{\text{Np}}$  and  $\delta^{13}\text{C}_{\text{Tq}}$  records point to highly variable conditions in near surface and subsurface water masses (Fig. 7d–f). This may indicate that the stratification could have been associated with proximity of the sea-ice margin.

5

#### 4.2.2 ~400 – ~800 AD, the Dark Ages Cold Period, DACP

The concentration of planktic foraminifera decreases and the percentages of *T. quinqueloba* are low (Fig. 5f,g–j). Together with the dominance of the polar species *N. pachyderma*, this indicates change towards cold oceanic conditions (Fig. 4g–j). The mean shell weights of *N. pachyderma* and *T. quinqueloba* decrease, which indicate a deterioration of the calcification conditions for these species (Fig. 6a). At ~610 AD, the  $\text{SST}_{\text{Mg/Ca}}$  and the  $\text{SST}_{\text{TF}}$  show a ~1 °C drop in temperature of subsurface and surface water masses, compared to the previous period (Fig. 8a,c). The low  $\Delta\delta^{18}\text{O}_{\text{Np-Tq}}$  suggest reduced Atlantic Water influence in the subsurface to near surface (Fig. 8d).

At ~700 AD, the decrease in  $\Delta\delta^{18}\text{O}_{\text{Np-Tq}}$  and increase in  $\Delta\delta^{18}\text{O}_{\text{Tq-Gu}}$  indicate weaker Atlantic water inflow and freshening at the surface that possibly prevented vertical mixing (Fig. 8d,f). Although the less saline conditions in the near surface and surface are indicated by single data points, they are in agreement with other, low-resolution studies from the northern continental margin off western Svalbard and north-western Barents Sea that report stratification of surface water masses and cooler upper surface-water for the late Holocene in this region (Berben et al. 2014; Werner et al., 2016) (Fig. 1).

The  $\text{SST}_{\delta^{18}\text{ONp}}$  and  $\text{SST}_{\text{Mg/Ca}}$  deviate from each other in this interval. While  $\text{SST}_{\delta^{18}\text{ONp}}$  and  $\text{SST}_{\delta^{18}\text{OTq}}$  show fairly warm conditions, the  $\text{SST}_{\text{Mg/Ca}}$  shows cold conditions (Fig. 8a,c). This discrepancy might be linked to the salinity effect on Mg/Ca of the water masses in which, *N. pachyderma* migrates during its ontogeny (Spielhagen and Erlenkeuser, 1994; Schiebel and Hemleben, 2005).

The  $\delta^{18}\text{O}_{\text{Np}}$  and  $\delta^{18}\text{O}_{\text{Tq}}$  values are low at ~400–600 AD and increase towards the present (Fig. 7Ia,b). In contrast, the  $\delta^{18}\text{O}_{\text{Gu}}$  show relatively constant values suggesting no change in isotopic composition of the surface water masses possibly indicating stratification of the surface water masses (Fig. 7Ic).

30

#### 4.2.3 ~800 – ~1400 AD, the Medieval Warm Period, MWP

The concentration of planktic foraminifera reaches its maximum of the 2000-year long record (Fig. 4f). The cold species *N. pachyderma* decreases and the subpolar species show high percentages indicating a change to warm surface conditions (Fig. 4g–j). At ~900–1400 AD, the average ocean SST<sub>TF</sub> is ~5.9 °C (Fig. 8c). The near surface and subsurface water masses show warming between ~900 and ~1100 AD as indicated by SST<sub>Mg/Ca</sub> and SST<sub>δ<sup>18</sup>O</sub>. *N. pachyderma* and SST<sub>δ<sup>18</sup>O</sub> *T. quinqueloba* (Fig. 8a,b). Also, the high Δδ<sup>18</sup>O<sub>Np-Tq</sub> point to strong Atlantic water inflow at the time (Fig. 8d). All the proxies clearly suggest a dominance of Atlantic water masses and discernible warm and favourable sea surface conditions for planktic foraminifera at the core site.

The warming is also expressed by the gradual increase in mean shell weight of both size-fractions of *N. pachyderma* and *T. quinqueloba* combined with low shell fragmentation (Fig. 6a,b). In the north-eastern Fram Strait at 78 °N, high mean shell weights of *N. pachyderma*, low fragmentation and other dissolution proxies also suggests favourable sea surface conditions at this time (Zamelczyk et al., 2013).

During the MWP, the trend in δ<sup>13</sup>C in *N. pachyderma*, *T. quinqueloba* and *G. uvula* is fairly similar (Fig. 7d–f). This might indicate that the water masses at the surface, near surface and subsurface were similar with respect to ventilation and/or productivity (Figs. 7a–c, 8b–d). Low percentages of *G. uvula* and Δδ<sup>18</sup>O<sub>Tq-Gu</sub> point to well-mixed waters and absence of a low salinity water layer at the surface indicating ice-free conditions during most of the year. The δ<sup>18</sup>O values in the three species could point to that the water column remained thermally stratified most of the time, even during the time of strongest inflow of Atlantic Water at ~900–1100 AD as indicated by high Δδ<sup>18</sup>O<sub>Np-Tq</sub>, SST<sub>TF</sub> and SST<sub>δ<sup>18</sup>O</sub><sub>Tq</sub> (Figs. 7a–c, 8b–d).

The period between ~1300 and ~1500 AD is characterized by fairly large changes in most proxies suggesting highly variable subsurface, near surface and surface water conditions. Shifts in all reconstructed SSTs, δ<sup>18</sup>O and δ<sup>13</sup>C values, as well as the short lasting stratification as indicated by the Δδ<sup>18</sup>O<sub>Tq-Gu</sub> and increased relative abundance of *G. uvula* point to an enhanced influence of melt water at the surface (Figs. 7I, 8e,f). This was probably caused by increase in sea-ice cover during winters initiated by the transition to the cooler sea surface conditions of the LIA. A similar transition from the MWP to the LIA interrupted by abrupt decadal-scale warmings, is commonly recognized in the proxy records in the Arctic and Subarctic region (see Werner et al., 2017).

#### 4.2.4 ~1400 – ~1950 AD, the Little Ice Age, LIA

The decrease of foraminiferal concentration to a minimum of the last 2000 years in addition to dominance of the polar species *N. pachyderma* indicate cold conditions during the LIA (Fig. 4f,g). At ~1400–1700 AD, the mean shell weight first decreased and at ~1550–1700 AD, it reached high values (few data points) (Fig. 6a). At ~1520 AD, the % fragmentation was high indicating dissolution (Fig. 6b). However, this seems unlikely, as the %TOC and %CaCO<sub>3</sub> remained stable and instead could be related to changes in [CO<sub>3</sub><sup>2-</sup>] and  $\Omega_{Ca}$  due to sea-ice melting during peak reproduction months in summers (Manno et al., 2012; Fransson et al., 2013). This is supported by the ~1.3 °C temperature drop in surface water masses indicated by SST<sub>TF</sub> (Fig. 8c). Whereas the surface experienced a cooling, the near surface and subsurface water masses warmed as shown by the increased SST <sub>$\delta^{18}O_{Tq}$</sub>  and SST<sub>Mg/Ca</sub>, respectively indicating continued flow of Atlantic water below a firmly stratified surface (Fig. 8a,b). The Atlantic water inflow was strong, as indicated by the high  $\Delta\delta^{18}O_{Np-Tq}$ , providing calcium carbonate-rich, well-saturated water masses (Fig. 8d) and possibly amplifying sea-ice melting.

The time interval ~1600–1800 AD, was characterized by slightly higher concentration of planktic foraminifera, lower percentages of *N. pachyderma*, relatively high relative abundances of subpolar species (*T. quinqueloba*, *G. uvula*, *N. incompta*) and high shell weights indicating warming of the surface ocean (Figs. 4f–j, 6a). The SST<sub>TF</sub> were at the same level as the SST<sub>TF</sub> during the MWP pointing to warm surface conditions (Fig. 8c). However, the inflow of Atlantic water diminished as indicated by the high  $\Delta\delta^{18}O_{Np-Tq}$  and the near surface and subsurface water masses experienced a slight cooling indicated by SST <sub>$\delta^{18}O_{Tq}$</sub>  and SST<sub>Mg/Ca</sub>, respectively (Fig. 8a,b,d). In the end of the warm phase, at ~1790 AD, the  $\Delta\delta^{18}O_{Tq-Gu}$  indicate increased stratification (Fig. 8f). The following interval at ~1800–1950 AD was characterized by the lowest SST of the past two millennia (Fig. 8a–c).

Between ~1800 and ~1950 AD, a shift to very low foraminiferal concentrations with dominance of *N. pachyderma* (up to 88%), very low mean shell weights and high %fragmentation and markedly increased IRD concentrations indicate the change to harsh ocean conditions with enhanced sea-ice and iceberg rafting (Figs. 4a,b,f,g, 6a,b). The lowest SST (SST<sub>TF</sub> ~2 °C, SST<sub>Mg/Ca</sub> ~3.3 °C, SST <sub>$\delta^{18}O_{Tq}$</sub> , ~3.1 °C) and percentages of subpolar species point to minimum ocean temperatures during the past 2000 years (Figs. 4h–j, 8a–c). The high  $\delta^{18}O$  and  $\delta^{13}C$  values of *N. pachyderma*, *T. quinqueloba* and *G. uvula*, may suggest a common

depth habitat indicative of permanent or near-permanent sea-ice cover. The foraminifera may migrate to better ventilated, nutrient-rich surface waters under such conditions (Volkman, 2000) (Fig. 7I).

#### 5 4.2.5 The last century ~1950 AD to present (2012)

Since ~1950 AD, the foraminiferal concentration and the percentages of *T. quinqueloba* and *G. uvula* increased gradually towards the present indicating continued warming (Fig. 4h–j). At the core top, the relative abundance of the cold species *N. pachyderma* decreases to a minimum of the entire record (Fig. 4g). Although the  $\Delta\delta^{18}\text{O}_{\text{Np-Tq}}$  indicate low Atlantic water inflow, the sea surface conditions during the last century clearly experienced warming, as indicated by  $\text{SST}_{\text{TF}}$  (Fig. 8c,d). The highest relative abundance of *G. uvula* and high IRD deposition suggest freshening of the surface, but without stratification as indicated by low  $\Delta\delta^{18}\text{O}_{\text{Tq-Gu}}$  (Figs. 4a,i, 8e,f). While the surface of the past ~60 years reaches a maximum of ~7 °C, (average 5.4 °C) as indicated by  $\text{SST}_{\text{TF}}$ , the temperatures of the near surface and subsurface water increase only slightly, as indicated by  $\text{SST}_{\text{Mg/Ca}}$  and  $\text{SST}_{\delta^{18}\text{O}}$  (Fig. 8a–c).

The surface warming is expected to correlate with an increase in shell weights of *N. pachyderma* and *T. quinqueloba*. However, the mean shell weights show only a slight weight increase and no change in %fragmentation (Fig. 6a,b). It has been shown that temperature and carbonate saturation play an important role in the calcification of foraminiferal shells (Russell et al., 2004; Lombard et al., 2010; Manno et al., 2012). Under low concentration of  $[\text{CO}_3^{2-}]$ , shell calcification rates tend to decrease (Manno et al., 2012). This can be linked to the recent ocean acidification where increase in  $\text{CO}_2$  in the ocean leads to a decrease of  $[\text{CO}_3^{2-}]$  and lower calcium-carbonate saturation (e.g. Chierici et al., 2011)

### 4.3 Comparison to other studies

The warm surface conditions identified in the core HH12-1206BC from Storfjorden Fan during the RWP, MWP and the last century are in agreement with numerous studies from the continental margin off western Svalbard, the western Barents Sea margin and northern North Atlantic Ocean (e.g., Sarnthein et al., 2003; Majewski et al., 2009; Spielhagen et al., 2011; Werner et al., 2011, 2016; Müller et al. 2012; Zamelczyk et al., 2013; Dylmer et al.,

2013; Berben et al. 2014; Pathirana et al., 2015; Moffa-Sánchez and Hall, 2017; Matul et al., 2018). It varies which of these periods show highest SST depending on the microfossil group studied (Matul et al., 2018). Nevertheless, in all studies the conditions of the warm periods are mainly attributed to higher intensity and volume of Atlantic water inflow.

5           At the western Svalbard continental margin the RWP correlates with high planktic foraminiferal flux and increased subsurface temperatures (Werner et al., 2011) and high phytoplankton biomarker content (~340 AD) (Müller et al., 2012). These changes are indicative for warming of the ocean linked to a northward retreat of the sea-ice edge due to strengthened Atlantic water inflow and/or changes in the atmospheric circulation pattern  
10 (Werner et al., 2011; Müller et al., 2012) (Fig. 1). This is supported by similarly warm SST and peak in relative abundance of *T. quinqueloba* in core 23258 from the western Barents Sea margin at ~280 AD, also attributed to a pulse of warm Atlantic Water advection (Sarnthein et al., 2003) (Fig. 1). A recent study based on diatom abundances by Matul et al. (2018) reports the RWP (46–455 AD) as a long period of warm sea surface conditions. Data from the  
15 subpolar gyre south of Denmark Strait, indicate enhanced influence of warm and salty Atlantic Waters inferred from high differences between  $\delta^{18}\text{O}$  measured on *N. pachyderma* and *T. quinqueloba*, low relative abundance of *N. pachyderma* together with reduced sea-ice cover (Moffa-Sánchez and Hall, 2017).

          The second warm period, the MWP recorded at Storfjorden Fan at ~400–1400 AD  
20 correlates well with foraminifera- and diatom-based climate reconstructions from the western Svalbard margin (Werner et al., 2011; Zamelczyk et al., 2013; Matul et al., 2018) and around Iceland (Moffa-Sánchez and Hall, 2017), and is explained by the strengthened inflow of Atlantic Water and ice-free winters. In the northern Barents Sea, the MWP is characterized by changes in composition of coccolithophore assemblages together with a significant increase in  
25 primary productivity and is also linked to increased influence of Atlantic-derived water masses (Dylmer et al., 2013; Pathirana et al., 2015) (Fig. 1). Moreover, numerous studies have documented warmer sea surface conditions as a local expression of a widely occurring warming since ~900 AD in the North Atlantic (e.g., Dahl-Jensen et al., 1998; Andersson et al., 2003; Moberg et al., 2005; Miettinen et al., 2015). The Arctic surface air temperature  
30 (SAT) reconstruction and the Northern Hemisphere spatial SAT identify the MWP as a ~300 year-long warm interval from 950 to ~1250 AD (Mann et al., 2009; Kaufman et al., 2009). The Summit station  $\delta^{18}\text{O}$  data at 950 AD show contemporary warmer temperatures in Greenland (Vinther et al., 2010). Overall, the patterns of reconstructed proxies in core HH12-

1206BC agree very well with the spatial SAT reconstruction by Mann et al. (2009) for the MWP. A distinct temperature anomaly in the SAT reconstructions of Mann (2009) for the entire Northern Hemisphere is also recorded in our Storfjorden Fan core seen as a clear temperature drop ~1300–1450 AD (Fig.8a-c).

5           The two cold periods, the DACP and the LIA (~400–800 AD and ~1400–1950 AD in the Storfjorden Fan record, respectively) from western Svalbard and Barents Sea margin correlate with pronounced changes in composition of planktic foraminiferal faunas, low planktic foraminiferal flux and presence of cold-water dinocyst assemblages linked to increased sea-ice cover and reduced influence of Atlantic water inflow and proximity of the polar front (Bonnet et al., 2010; Berben et al. 2014; Werner et al., 2011; 2016). During the DACP, similar conditions with low primary productivity have also been reported for the northern Barents Sea before 750 AD and have been associated with reduced inflow of waters from the Nordic seas and a southeastward shift of the marginal ice zone (Pathirana et al., 2015).

15           The warmer period within the LIA ~1600–1800 AD in the Storfjorden Fan record, has also been reported in studies from the North Atlantic at 1600–1820 AD (Miettinen et al., 2015) and at 1700–1800 AD (e.g., Mann et al., 2009). On the western Svalbard margin, high sea surface salinity also indicates enhanced Atlantic water influence at ~1600 AD (Werner et al., 2011). As the salinity increase was not accompanied by warmer temperatures, these salinity values were considered as erroneous (Werner et al., 2011).

20           Numerous paleoproxy studies suggest a progressive warming over the last ~200 years in the Arctic region (e.g., Kaufman et al., 2009; Majewski et al., 2009; Spielhagen et al., 2011; Werner et al., 2011; Zamelczyk et al., 2013; Dylmer et al., 2013). Some studies consider the last 100 years as the warmest period of the last two millennia (Spielhagen et al., 25 2011; Werner et al., 2011), although preservation issues with improved preservation in surface sediments may have biased results (Zamelczyk et al., 2013). At Storfjorden Fan, the SST<sub>TF</sub> reconstructions show a distinct warming trend at the surface from 1950 AD onwards, while the SST<sub>Mg/Ca</sub> and the  $\delta^{18}\text{O}$  on *N. pachyderma* and *T. quinqueloba* do not show any near- or subsurface warming. This inconsistency might be linked to a different source and/or 30 mechanism for the thermal change in the water masses or preservation.

#### 4.4 Solar irradiance - driver of short-scale changes in sea surface conditions in the late Holocene?

The environmental controls of the marine paleoclimate at Storfjorden Fan and the west Spitsbergen margin during the late Holocene are clearly a function of the strength of the Atlantic water inflow to the Fram Strait and the proximity of the sea-ice margin (e.g., Risebrobakken et al., 2003; 2011; Hald et al., 2007; Rasmussen et al., 2007, 2014; Majewski et al., 2009; Zamelczyk et al., 2013; Aagaard-Sørensen et al., 2014; Berben et al., 2014; Werner et al., 2013, 2016; Łacka et al., 2015; Telesiński et al., 2017; this study). However, several previous studies suggested significant influence of solar irradiance on North Atlantic climate throughout the Holocene (Lamb, 1979; Bond et al., 2001).

10 We compare our foraminiferal sea surface temperatures at 10 m water depth based on transfer functions and the relative abundances of the surface dwelling *G. uvula* with the total solar irradiance (TSI) reconstructed from  $^{10}\text{Be}$  in Antarctic and Greenland ice cores (Steinhilber et al., 2012). Despite of some differences in the age models, the timing of SST shifts at Storfjorden Fan show a fairly close correlation with total solar irradiance variability superimposed on the large-scale, multi-centennial warm and cold periods, that correlate with the well-known climatic events of the last two millennia (RWP, DACP, MWP, LIA) (Fig. 9).  
15 Most of the phases of solar minima correlate with low SST and low percentages of *G. uvula* and vice versa (Fig. 9a–c).

The Subpolar Gyre is considered a dominant large-scale feature of the surface circulation of the North Atlantic (Hatun et al., 2005; Hoggins et al., 2011). In the Iceland Basin, Moffa-Sánchez et al. (2014) reconstructed SST and salinity using paired  $\delta^{18}\text{O}$  and Mg/Ca data on the planktic foraminiferal species *Globorotalia inflata*, together with climate-model simulations. The authors suggest a strong correlation between SST and TSI over the past 1000 years linked to the strength of the Subpolar Gyre. Jiang et al. (2015) shows equally  
25 strong correlation between SST based on diatom assemblages and TSI, which further supports the SST-TSI linkage in the subpolar region. Numerous modeling studies postulate a strong influence of the Subpolar Gyre also on the Atlantic water inflow to the Nordic seas, the Fram Strait and the Barents Sea (Karcher et al. 2003; Hatun et al., 2005; Lohmann et al., 2009).

The correlation of sea surface temperatures recorded by planktic foraminifera at  
30 Storfjorden Fan to known TSI anomalies of the last 2000 years imply that solar activity could have had a dominant influence on sea surface conditions on short decadal to multi-decadal scales (Fig. 9b,c). Moreover, the link between the high relative abundance of *G. uvula*, a low-salinity species, and high TSI suggest an influence of solar irradiance on the intensity of

stratification formed most likely by solar heating of the upper ocean layers (Fig. 9a,c).

However, the different resolutions of the two records hamper a precise comparison and make it impossible to determine the forcing of sea surface condition changes at the HH12-1206BC site. Despite this hindrance, the results might suggest that at least over the last two millennia solar forcing, possibly amplified by atmospheric forcing, has been responsible for the short-term variability of the surface conditions superimposed on the multi-centennial warm and cold periods at Storfjorden Fan.

Despite the increasing numbers of paleorecords proposing a TSI-Holocene SST connection in high-latitude regions of the North Atlantic (Bond et al., 2001; Jiang et al., 2015; Moffa-Sanchez et al., 2014) as well as of the North Pacific (Clegg et al., 2011; Tinner et al., 2015), the linkage of late Holocene climate change to solar irradiance is controversial as several studies have invoked volcanism as a considerably more important factor e.g., during the LIA (Hegerl et al., 2003; Miller et al., 2012). Other studies considered both volcanic and solar forcings responsible for the global mean LIA signal, but emphasized that the volcanic forcing was a major player in global-scale cooling, while the solar variability was a major player in regional changes and extreme cold events (Shindell et al., 2003).

Until recently, sea surface temperatures and climate variability on multi-decadal timescales were largely believed to be controlled by internal processes rather than external forcing. However, the foraminiferal SST-TSI correlation suggest that the solar variability is affecting short-term sea surface conditions through ocean-atmosphere links not only in the area of the Supolar Gyre, but also further north in the northern Fram Strait. This potential linkage warrants further research in order to understand this component of natural climate variability, which apparently exerts an essential influence on the northern North Atlantic climate system.

## 5 Conclusions

The major climate anomalies of the past two millennia were reflected in planktic foraminiferal records at Storfjorden Fan, western Svalbard margin (distribution of species, SST reconstructions by Mg/Ca, transfer functions and  $\delta^{18}\text{O}$  and  $\delta^{13}\text{C}$  values of *Neogloboquadrina pachyderma*, *Turborotalita quinqueloba* and *Globigerinita uvula*). The oceanic conditions at ~400–800 AD and ~1400–1950 AD were associated with the local

expression of the Dark Age Cold Period (DACP) and the Little Ice Age (LIA), respectively. They are characterized by low concentrations of planktic foraminifera, low relative abundances of subpolar species and dominance of the polar species *N. pachyderma*. The surface (30–0 m) conditions were cold, but although the Atlantic water influence diminished, the near surface (100–30 m) and subsurface (250–100 m) showed relatively high temperatures. During the LIA, the period ~1600–1800 AD, was relatively warm, but followed by the coldest interval of the past two millennia at ~1800–1950 AD.

High concentration of planktic foraminifera, high percentages of subpolar species and decreased relative abundances of *N. pachyderma*, with high mean shell weights and high temperatures characterized periods at ~0–400 AD, ~800–1400 AD and from ~1950 AD to the present. These periods were linked to the RWP, MWP and the most recent warming, respectively.

The reconstructed properties and structure of the water column seem to be a function of the inflow of Atlantic water masses and presence of sea ice as well as the variability of the location of the sea-ice margin and the Arctic Front. Strongest Atlantic water inflow and highest temperatures in the upper water column (subsurface, near surface and surface) occurred during MWP at ~900–1100 AD.

Stratification of the surface water masses, inferred from trends in the  $\delta^{18}\text{O}$  values measured on the surface-dwelling *G. uvula*, near-surface dwelling *T. quinqueloba* and subsurface-living *N. pachyderma* likely persisted over the past 2000 years. This is in agreement with other studies, which postulate stratification reinforcement of climate trends during the Late Holocene.

Short-lasting minima of SST calculated by transfer functions and decreased relative abundance of *G. uvula*, the low-salinity species, are in near-phase with solar minima. These short-lasting changes are superimposed on the large-scale, multi-centennial warm and cold periods that correlate with the above-mentioned, well-known climatic events of the last two millennia and imply that solar forcing has been responsible for decadal to multi-decadal sea surface variability over the Storfjorden Fan over the last two millennia.

*Data availability.* The foraminifera data set will be made publicly available on PANGAEA online data archives.

*Author contributions.* KZ performed the core processing and foraminifera analyses and initiated the study together with TLR. MR provided the trace element data and MC carried out water carbonate chemistry analyses. All authors discussed and edited the manuscript.

5 *Competing interests.* The authors declare that they have no conflict of interest.

## Acknowledgements

10 We thank the captains and crews of *RV Jan Mayen/Helmer Hanssen* and S. Iversen and B.R. Olsen for technical assistance by retrieving the sediment core. T. Dahl is thanked for laboratory assistance and T. Grytå for creating the area map. We thank B. Sternal and W. Szczuciński for helpful suggestions and discussions of interpretation of the  $^{210}\text{Pb}$  and  $^{137}\text{Cs}$  dating. We also thank two anonymous reviewers for their helpful comments which greatly  
15 improved the manuscript. The study was carried out within the framework of the project „Effects of ocean chemistry changes on planktic foraminifera in the Fram Strait: Ocean Acidification from natural to anthropogenic changes” funded by The Research Council of Norway (project number 216538), the Centre for Arctic Gas Hydrate, Environment and Climate (CAGE), UiT supported by the Research Council of Norway, project number 223259  
20 and the Arctic University of Norway, Tromsø.

## References

- 25 Aagaard Sørensen, S., Husum, K., Werner, K., Spielhagen, R. F., Hald, M. and Marchitto, T. M.: A late glacial-early Holocene multiproxy record from the eastern Fram Strait, Polar North Atlantic, *Mar. Geol.*, 355, 15–26, 2014a.
- Andersson, C., Risebrobakken, B., Jansen, E. and Dahl, S. O.: Late Holocene surface ocean conditions of the Norwegian Sea (Voring Plateau), *Paleoceanography*, 18 (1044), 13, 2003.
- 30 Barker, S. and Elderfield, H.: Foraminiferal calcification response to glacial- interglacial changes in atmospheric  $\text{CO}_2$ , *Science*, 297, 833, 2002.
- Barker, S., Greaves, M. and Elderfield, H.: A study of cleaning procedures used for foraminiferal Mg/Ca paleothermometry, *Geochem., Geophys., Geosys.*, 4(9) 8407, 2003.

- Barker, S., Kiefer, T. and Elderfield, H.: Temporal changes in North Atlantic circulation constrained by planktonic foraminiferal shell weights, *Paleoceanography*, 19, 2004.
- Bauch, D., Carsens, J. and Wefer, G.: Oxygen isotope composition of living *Neogloboquadrina pachyderma* (sin.) in the Arctic Ocean, *Earth Planet. Sc. Lett.*, 146, 47–58, 5 1997.
- Bemis, B. E., Spero, H. J., Lea, D. W. and Bijma, J.: Temperature influence on the carbon isotopic composition of *Globigerina bulloides* and *Orbulina universa* (planktonic foraminifera), *Mar. Micropaleontol.*, 38, 213–228, 2000.
- 10 Berben, S., Husum, K., Cabedo-Sanz, P. and Belt, S. T.: Holocene sub-centennial evolution of Atlantic water inflow and sea ice distribution in the western Barents Sea, *Clim. Past*, 10, 181–198, 2014.**
- Bergami, C., Capotondi, L., Langone, L., Giglio, F. and Ravaioli, M.: Distribution of living planktonic foraminifera in the Ross Sea and the Pacific sector of the Southern Ocean (Antarctica), *Mar. Micropaleontol.*, 73, 37–48, 2009.
- 15 Berger, W. H.: Planktonic foraminifera- selective solution and the lysocline, *Mar. Geol.*, 8(2), 111–138, 1970.
- Berger, W. H., Bonneau, M. C. and Parker, F. L.: Foraminifera on the deep-sea floor: lysocline and dissolution rate, *Oceanol. Acta*, 5, 249–258, 1982.
- Bianchi, G. G. and McCave, I. N.: Holocene periodicity in North Atlantic climate and deep- 20 ocean flow south of Iceland, *Nature*, 397, 515–517, 1999.
- Birch, H. S., Coxall, H. K., Pearson, P. N, Kroon, D. and O’Regan, M.: Planktonic foraminifera stable isotopes and water column structure: Disentangling ecological signals, *Mar. Micropaleontol.*, 101, 127–145, 2013.
- Blindheim, J., Borovkov, V., Hansen, B., Malmberg, S. A, Turrell, W. R., and Østerhus, S.: 25 Upper layer cooling and freshening in the Norwegian Sea in relation to atmospheric forcing, *Deep-Sea Res., Part I* 47(4), 655–680, 2000.
- Boltovskoy, E., Boltovskoy, D., Correa, N., and Brandini, F.: Planktic foraminifera from the southwestern Atlantic (30–60 °S): species-specific patterns in the upper 50 m, *Mar. Micropaleontol.*, 28, 53–72, 1996.
- 30 Boltovskoy, E. and Lena, H.: Seasonal occurrences, standing crop and production in benthic foraminifera of Puerto Deseado, Cushman Found, *Foram. Res.*, 20, 87, 1970b.

- Bond, G., Kromer, B., Beer, J., Muscheler, R., Evans, M. N., Showers, W., Hoffmann, S., Lotti-Bond, R., Hajdas, I. and Bonani, G.: Persistent solar influence on North Atlantic climate during the Holocene, *Science*, 294(5549), 2130–2136, 2001.
- Bonnet, S., de Vernal, A., Hillaire-Marcel, C., Radi, T. and Husum, K.: Variability of  
5 seasurface temperature and sea-ice cover in the Fram Strait over the last two millennia, *Mar. Micropaleontol.*, 74, 59–74, 2010.
- Brambilla, E., Talley, L. D. and Robbins, P. E.: Subpolar Mode Water in the northeastern Atlantic: 2. Origin and transformation, *J. Geophys. Res.*, 113, 2008.
- Carstens, J., Hebbeln, D. and Wefer, G.: Distribution of planktic foraminifera at the ice  
10 margin in the Arctic (Fram Strait), *Mar. Micropaleontol.*, 29, 257–269, 1997.
- Chierici, M. and Fransson, A.: CaCO<sub>3</sub> saturation in the surface water of the Arctic Ocean: Undersaturation in freshwater influenced shelves, *Biogeoscience*, 6, 2421–2431, 2009.
- Chierici, M., Fransson, A., Lansard, B., Miller, L.A., Mucci, A., Shadwick, E., Thomas, H., Tremblay, J-E. and Papakyriakou, T.: The impact of biogeochemical processes and  
15 environmental factors on the calcium carbonate saturation state in the Circumpolar Flaw Lead in the Amundsen Gulf, Arctic Ocean, *J. Geophys. Res.: Oceans*, 116, 2011.
- Clegg, B. F., Kelly, R. and Clarke, G. H.: Nonlinear response of summer temperature to Holocene insolation forcing in Alaska, *Proc. Nat. Acad. Sci.*, 108(48), 19299–19304, 2011.
- Coxall, H. K., Wilson, P. A., Pearson, P. N. and Sexton, P. E.: Iterative evolution of digitate  
20 planktonic foraminifera, *Paleobiol.*, 33(4), 495–516, 2007.
- Dahl-Jensen, D., Mosegaard, K., Gundestrup, N., Clow, G. D., Johnsen, S. J., Hansen, A .W. and Balling, N.: Past temperatures directly from the Greenland Ice Sheet, *Science*, 282, 268–271, 1998.
- Dickson, A. G.: Standard potential of the (AgCl(s)11/2H<sub>2</sub> (g)5Ag(s)1HCl(aq)) cell and the  
25 dissociation constant of bisulfate ion in synthetic sea water from 273.15 to 318.15 K, *J. Chem. Thermodyn.*, 22, 113–127, 1990.
- Dickson, A. G., Sabine, C. L. and Christian, J. R.: Guide to best practices for ocean CO<sub>2</sub> Measurements, *PICES Sp. Pub.*, 3, 191, 2007.
- Dickson, A. G. and Millero, F. J.: A comparison of the equilibrium constants for the  
30 dissociation of carbonic acid in seawater media, *Deep Sea Res.*, 34, 1733–1743, 1987.
- Dokken, T. and Hald, M.: Rapid climatic shifts during isotope stages 2–4 in the Polar North Atlantic, *Geology*, 7, 599–602, 1996.

- Duplessy, J.-C.: Isotope studies. In: Gribbin J. (ed) Climatic change, Cambridge Univ Press, London, 46–67, 1978.
- Dylmer, C. V., Giraudeau, J., Eynaud, F., Husum, K. and de Vernal, A.: Northward advection of Atlantic water in the eastern Nordic Seas over the last 3000 year, *Clim. Past*, 9, 1505–1518.
- 5 Eddy, J. A.: The maunder minimum, *Science*, 192, 1189–1202, 1978.
- Emiliani, C.: Depth habitats of some species of pelagic foraminifera as indicated by oxygen isotope ratios, *Am. J. Sci.*, 252, 149–158, 1954.
- Erez, J.: Vital effect on stable-isotope composition seen in foraminifera and coral skeletons, *Nature*, 273(5659), 199–202, 1978.
- 10 Espitalié, J., Laporte, J. L., Madec, M., Marquis, F., Leplat, P., Paulet, J. and Boutefeu, A.: Méthode rapide de caractérisation des roches-mères, de leur potentiel pétrolier et de leur degré d'évolution, *Revue de l'Institut Français du Pétrole*, 32, 23–42, 1977.
- Ezard, T. H. G., Edgar, K. M. and Hull, P. M.: Environmental and biological controls on size-specific  $\delta^{13}\text{C}$  and  $\delta^{18}\text{O}$  in recent planktonic foraminifera, *Paleoceanography*, 30, 151–173,
- 15 2015.
- Feyling-Hanssen, R. W., Jorgensen, J. A., Knudsen, K. L. and Anderson, A. L.: Late Quaternary Foraminifera from Vendsyssel, Denmark and Sandnes, Norway, *Bull. Geol. Soc. Den.*, 21, 67–317, 1971.
- Fransson, A., Chierici, M., Miller, L. A., Carnat, G., Thomas, H., Shadwick, E., Pineault, S.
- 20 and Papakyriakou, T. M.: Impact of sea ice processes on the carbonate system and ocean acidification state at the ice-water interface of the Amundsen Gulf, Arctic Ocean, *J. Geophys. Res.: Oceans*, 118, 1–23, 2013.
- Fogel, M. L. and Cifuentes, L. A.: Isotope fractionation during primary production. In *Org. Geochem.*, eds. M. H. Engel and S.A. Macko (New York, NY: Plenum Press), 1993.
- 25 Giraudeau, J., Grelaud, M., Solignac, S., Andrews, J. T., Moros, M., and Jansen, E.: Millennial-scale variability in Atlantic water advection to the Nordic Seas derived from Holocene coccolith concentration records, *Quat. Sci. Rev.*, 29(9–10), 2010.
- Grove, J. M.: *Little Ice Ages: Ancient and Modern*, (2 volumes), London, 718, 2004.
- Hald, M., Andersson, C., Ebbesen, H., Jansen, E., Klitgaard Kristensen, D., Risebrobakken,
- 30 B., Salomonsen, G. R., Sarnthein, M., Sejrup, H. P. and Telford, R. J.: Variations in temperature and extent of Atlantic water in the northern North Atlantic during the Holocene, *Quat. Sci. Rev.*, 26, 3423–3440, 2007.

- Hathorne, E. C., Gagnon, A., Felis, T., Adkins, J., Asami, R., Boer, W., Caillon, N., et al.: Interlaboratory study for coral Sr/Ca and other element/Ca ratio measurements, *Geochem., Geophys., Geosys.*, 14, 3730–3750, 2013.
- Hatun, H., Sandø, A-B., Drange, H., Hansen, B. and Valdimarsson, H.: Influence of the Atlantic subpolar gyre on the thermohaline circulation, *Science*, 309, 1841–1844, 2005.
- Hebbeln, D., Henrich, R. and Baumann, K. H.: Paleoceanography of the last interglacial/glacial cycle in the polar North Atlantic, *Quat. Sci. Rev.*, 17, 125–153, 1998.
- Hegerl, G. C., Crowley, T. J., Baum, S. K., Kim, K.-Y. and Hyde W. T.: Detection of volcanic, solar and greenhouse gas signals in paleo-reconstructions of Northern Hemispheric temperature, *Geophys. Res. Lett.*, 30(5), 1242, 2003.
- Hemleben, Ch., Spindler, M. and Anderson, O. R.: *Modern Planktonic Foraminifera*, Springer-Verlag, New York, 363, 1989.
- Higginson, S., Thompson, K. R., Huang, J., Veronneau, M. and Wright, D. G.: The mean surface circulation of the North Atlantic subpolar gyre: a comparison of estimates derived from new gravity and oceanographic measurements, *J. Geophys. Res.: Oceans*, 116, 2011.
- Hoff, U., Rasmussen, T. L., Stein, R. M., Ezat, M. and Fahl, K.: Sea ice and millennial-scale climate variability in the Nordic seas 90 ka to present. *Nature Comm.*, 7, 12247, 2016.
- Hulot, V.: Variabilité spatiale et structurelle des communautés du phytoplancton et de foraminifères planctoniques à l'entrée de la Mer de Barents, Msc thesis, Université de Bretagne Occidentale, 2015.
- Husum, K. and Hald, M.: Arctic planktic foraminiferal assemblages: implications for subsurface temperature reconstructions, *Mar. Micropaleontol.*, 96–97, 38–47, 2012.
- Huber, R., Meggers, H., Baumann, K. H. and Henrich, R.: Recent and Pleistocene carbonate dissolution in sediments of the Norwegian-Greenland Sea, *Mar. Geol.*, 165, 123–136, 2000.
- Inoue, M., Nohara, M., Okai, T., Suzuki, A. and Kawahata, H.: Concentrations of Trace Elements in Carbonate Reference Materials Coral JCp-1 and Giant Clam JCt-1 by Inductively Plasma-Mass Spectrometry, *Geostand. Geoanalytic. Res.*, 28, 411–416, 2004.
- IPCC: Summary for policymakers, intergovernmental panel on climate change, *The Fifth Assessment Report*, IPCC, 2014.
- Jessen, S. P., Rasmussen, T. L., Nielsen, T. and Solheim, A.: A new Late Weichselian and Holocene marine chronology for the western Svalbard slope 30,000-0 cal years BP, *Quat. Sci. Rev.*, 29(9–10), 1301–1312, 2010.

- Jiang, H., Muscheler, R., Bjorck, S., Seidenkrantz, M.-S., Olsen, J., Sha, L., Sjolte, J., Eiriksson, J., Ran, L., Knudsen, K.-L. and Knudsen, M. F.: Solar forcing of Holocene summer sea-surface temperatures in the northern North Atlantic, *Geology*, 43(3), 203–206, 2015.
- Jonkers, L., Brummer, G.-J. A., Peeters, F. J. C., van Aken, H. M. and De Jong, M. F.:  
5 Seasonal stratification, shell flux, and oxygen isotope dynamics of left-coiling *N. pachyderma* and *T. quinqueloba* in the western subpolar North Atlantic, *Paleoceanography*, 25, 2010.
- Juggins, S.: Software for Ecological and Palaeoecological Data Analysis and Visualization. C2, Version 1.6.6. University of Newcastle upon Tyne, UK, 2010.
- Karcher, M. J., Gerdes, R., Kauker, F. and Köberle, C.: Arctic warming: Evolution and  
10 spreading of the 1990s warm event in the Nordic seas and the Arctic Ocean, *J. Geophys. Res.: Oceans*, 108, 3034, 2003.
- Kaufman, D. S., Schneider, D. P., McKay, N. P., Ammann, C. M., Bradley, R. S., Briffa, K. R. et al.: Recent warming reverses long-term Arctic cooling, *Science*, 325, 1236–1239, 2009.
- Knudsen, K. L.: Foraminiferer i Kvartær stratigrafi: Laboratorie og fremstillingsteknik samt  
15 udvalgte eksempler, *Geologisk Tidsskrift* 3, 1998.
- Kozdon, R., Eisenhauer, A., Weinelt, M., Meland, M. Y. and Nürnberg, D.: Reassessing Mg/Ca temperature calibrations of *Neogloboquadrina pachyderma* (sinistral) using paired  $\delta^{44}/^{40}\text{Ca}$  and Mg/Ca measurements, *Geochem., Geophys., Geosys.*, 10, 2009.
- Kunzendorf, H. and Larsen, B.: A 200–300 year cyclicity in sediment deposition in the  
20 Gotland Basin, Baltic Sea, as deduced from geochemical evidence, *Appl. Geochem.*, 17, 29–38, 2002.
- Lamb, H.: Climatic variation and changes in the wind and ocean circulation: The Little Ice Age in the northeast Atlantic, *Quat. Res.*, 11, 1–20, 1979.
- Lamb, H. H.: Climate: present, past and future, *Climatic History and the Future*, vol.2.  
25 Methuen & Co, 1977.
- Lohmann, G. P.: A model for variation in the chemistry of planktonic foraminifera due to secondary calcification and selective dissolution, *Paleoceanography*, 10 (3), 445–457, 1995.
- Lohmann, K., Drange, H. and Bentsen, M.: Response of the North Atlantic subpolar gyre to persistent North Atlantic oscillation like forcing, *Clim. Dyn.*, 32(2–3), 273–285, 2009.
- 30 Loeng, H.: Features of the physical oceanographic conditions of the Barents Sea, *Polar Res.*, 10, 5–18, 1991.

- Lombard, F., da Rocha, R. E., Bijma, J. and Gattuso, J.-P.: Effect of carbonate ion concentration and irradiance on calcification in planktonic foraminifera, *Biogeoscience*, 7, 247–255, 2010.
- Lutze, G. F. and Altenbach, A.: Technik und Signifikanz der Lebendfärbung benthischer Foraminiferen mit Bengalrot, *Geol. Jb. A.*, 128, 251–265, 1991.
- 5 Łącka, M., Zajaczkowski, M., Forwick, M. and Szczuciński, W.: Late Weichselian and Holocene paleoceanography of Storfjordrenna, southern Svalbard, *Clim. Past*, 11, 587–603, 2015.
- Maiti, K., Carroll, J. and Benitez-Nelson, C. R.: Sedimentation and particle dynamics in the seasonal ice zone of the Barents Sea, *J. of Mar. Sys.*, 79, 185–98, 2010.
- 10 Majewski, W., Szczuciński, W. and Zajaczkowski, M.: Interactions of Arctic and Atlantic water-masses and associated environmental changes during the last millennium, Hornsund (SW Svalbard), *Boreas*, 38, 529–544, 2009.
- Mangerud, J., Bondevik, S., Gulliksen, S., Hufthammer, A. K. and Høisæter, T.: Marine 14C reservoir ages for 19th century whales and molluscs from the North Atlantic, *Quat. Sci. Rev.*, 25, 3228–3245, 2006.
- 15 Mann, M. E., Zhang, Z., Rutherford, S., Bradley, R. S., Hughes, M. K., Shindell, D., Ammann, D. C., Faluvegi, G. and Ni, F.: Global signatures and dynamical origins of the Little Ice Age and Medieval Climate Anomaly, *Science*, 326, 1256–1260, 2009.
- 20 Manno, C., Morata, N. and Bellerby, R.: Effect of ocean acidification and temperature increase on the planktonic foraminifer *Neogloboquadrina pachyderma* (sinistral), *Polar Bio.*, 35, 1311–1319, 2012.
- Marnela, M., Rudels, B., Olsson, K. A., Anderson, L. G., Jeansson, E., Torres, D. J., Messias, M. J., Swift, J. H. and Watson, A.: Transports of Nordic Seas water masses and excess SF<sub>6</sub> through Fram Strait to the Arctic Ocean, *Prog. Oceanogr.*, 78(1), 1–11, 2008.
- 25 Matul, A., Spielhagen, F. R., Kazarina, G., Kruglikova, S., Dmitrenko, O. and Mohan, R.: Warm-water events in the eastern Fram Strait during the last 2000 years as revealed by different microfossil groups, *Polar Res.*, 37(1), 1540243, 2018.
- McKee, B. A., Nittrouer, C. A. and DeMaster, D. J.: Concepts of sediment deposition and accumulation applied to the continental shelf near the mouth of the Yangtze River, *Geology*, 30, 631–633, 1983.
- Meilland, J.: Rôle des Foraminifères planctoniques dans le cycle du carbone marin des hautes latitudes (Océan Indien Austral) (PhD Thesis), Angers University, France, 1–200, 2015.

- Meilland, J., Howa, H., LoMonaco, C. and Schiebel, R.: Individual planktic foraminifer protein-biomass affected by trophic conditions in the Southwest Indian Ocean, 30 °S–60 °S, *Mar. Micropaleontol.*, 124, 63–74, 2016.
- Mehrbach, C., Culberson, C. H., Hawley, J. E. and Pytkowicz, R. M.: Measurement of the  
5 apparent dissociation constants of carbonic acid in seawater at atmospheric pressure. *Lim. and Oceanog.*, 8, 897–907, 1973.
- Meredith, M., Heywood, K., Dennis, P., Goldson, L., White, R., Fahrbach, E., Schauer, U. and Østerhus, S. (2001). Freshwater fluxes through the Western Fram Strait. *Geophys. Res. Lett.*, 28(8), 1615–1618.
- 10 Miettinen, A., Divine, D. V., Husum, K., Koç, N. and Jennings, A.: Exceptional ocean surface conditions on the SE Greenland shelf during the Medieval Climate Anomaly, *Paleoceanography*, 30, 1657–1674, 2015.
- Miller, G. H., Geirsdóttir, Á., Zhong, Y., Larsen, D. J., Otto-Bliesner, B. L. et al: Abrupt onset of the Little Ice Age triggered by volcanism and sustained by sea-ice/ocean feedbacks,  
15 *Geophys. Res. Lett.*, 39, 2012.
- Moberg, A., Sonechkin, D. M., Holmgren, K., Datsenko, N. M. and Karlén, W.: Highly variable Northern Hemisphere temperatures reconstructed from low- and high- resolution proxy data, *Nature*, 433, 613–617, 2005.
- Moffa-Sánchez, P., Born, A., Hall, I. R., Thornalley, D. J. R and Barker, S.: Solar forcing of  
20 North Atlantic surface temperature and salinity over the past millennium, *Nature Geosci.*, 7(4), 275–278, 2014.
- Moffa-Sánchez, P. and Hall, I. R.: North Atlantic variability and its links to European climate over the last 3000 years, *Nature Comm.*, 8, 1726, 2017.
- Mucci, A.: The solubility of calcite and aragonite in seawater at various salinities,  
25 temperatures and at one atmosphere pressure, *Am. J. Sc.*, 283, 781–799, 1983.
- Müller, J., Massé, G., Stein, R. and Belt, S. T.: Variability of sea-ice conditions in the Fram Strait over the past 30,000 years, *Nature Geosci.*, 2 (11), 772–776, 2009.
- Müller, J., Werner, K., Stein, R., Fahl, K., Moros, M. and Jansen, E.: Holocene cooling  
culminates in sea-ice oscillations in Fram Strait, *Quat. Sci. Rev.*, 47, 1–14, 2012.
- 30 NSIDC: National Snow and Ice Data Center, 2018.
- Oppo, D. W., McManus, J. F. and Cullen, J. L.: Deepwater variability in the Holocene Epoch, *Nature*, 422, 277–278, 2003.

- Owrid, G., Socal, G., Civitarese, G., Luchetta, A., Wiktor, J., Nöthig, E. M., Andreassen, I., Schauer, U. and Strass, V.: Spatial variability of phytoplankton, nutrients and new production estimates in the waters around Svalbard, *Polar Res.*, 19, 155–171, 2000.
- Pados, T. and Spielhagen, R. F.: Species distribution and depth habitat of recent planktic foraminifera in Fram Strait, Arctic Ocean, *Polar Res.*, 33, 2014.
- Pados, T., Spielhagen, R. F., Bauch, D., Meyer, H. and Segl, M.: Oxygen and carbon isotope composition of modern planktic foraminifera and near-surface waters in the Fram Strait (Arctic Ocean) - a case study, *Biogeoscience*, 12, 1733–1752, 2015.
- Pathirana, I., Knies, J., Felix, M. and Mann, U.: Towards an improved organic carbon budget for the western Barents Sea shelf, *Clim. Past*, 10, 569–587, 2014.
- Pathirana, I., Knies, J., Felix, M., Mann, U. and Ellingsen, I.: Middle to late Holocene paleoproductivity reconstructions for the western Barents Sea: a model-data comparison, *Arktos*, 1, 20, 2015.
- Pawłowska, J., Zajączkowski, M., Łacka, M., Lejzerowicz, F., Esling P. and Pawłowski, J.: Palaeoceanographic changes in Hornsund Fjord (Spitsbergen, Svalbard) over the last millennium: new insights from ancient DNA, *Clim. Past*, 12, 1459–1472, 2016.
- Parker, F. L.: Planktonic Foraminiferal Species in Pacific Sediments, *Mar. Micropaleontol.*, 8, 219–254, 36, 1962.
- Peeters, F. J. C., Brummer, G. A. and Ganssen, G.: The effect of upwelling on the distribution and stable isotope composition of *Globigerina bulloides* and *Globigerinoides ruber* (planktic foraminifera) in modern surface waters of the NW Arabian Sea, *Glo. Planet. Change*, 34, 269–291, 2002.
- Pierrot, D., Lewis, E. and Wallace, D. W. R.: MS excel program developed for CO<sub>2</sub> system calculations, ORNL/CDIAC-105, Carbon Dioxide Information Analysis Center, Oak Ridge National Laboratory, U.S. Department of Energy, Oak Ridge, 2006.
- Rasmussen, T. L., Thomsen, E., Ślubowska, M. A., Jessen, S., Solheim, A. and Koç N.: Paleooceanographic evolution of the SW Svalbard margin (76°N) since 20,000 14C yr BP, *Quat. Res.*, 67(1), 100–114, 2007.
- Rasmussen, T. L., Thomsen, E., Skirbekk, K., Ślubowska-Woldengen, M., Klitgaard Kristensen, D. and Koç, N.: Spatial and temporal distribution of Holocene temperature maxima in the northern Nordic seas: interplay of Atlantic, Arctic and polar water masses, *Quat. Sci. Rev.*, 92, 280–291, 2014.

- Ravelo, A. C. and Fairbanks, R. G.: Oxygen isotopic composition of multiple species of planktonic foraminifera: Recorders of the modern photic zone temperature gradient, *Paleoceanography*, 7(6), 815–831, 1992.
- Ravelo, A. C. and Fairbanks R. G.: Carbon isotopic fractionation in multiple species of planktonic foraminifera from core-tops in the tropical Atlantic, *J. Foram. Res.*, 25(1), 53–74, 1995.
- Rebotim, A., Voelker, A. H. L., Jonkers, L., Waniek, J. J., Meggers, H., Schiebel, R., Fraile, I., Schulz, M. and Kucera, M.: Factors controlling the depth habitat of planktonic foraminifera in the subtropical eastern North Atlantic, *Biogeoscience*, 14 (4), 827, 2017.
- 10 Reimer, P. J., Bard, E., Bayliss, A., Beck, J. W. et al.: IntCal13 and Marine13 radiocarbon age calibration curves, 0–50,000 years cal BP, *Radiocarbon*, 55 (4), 1869–1887, 2013.
- Risebrobakken, B., Jansen, E., Andersson, C., Mjelde, E. and Hevrøy, K.: A high resolution study of Holocene paleoclimatic and paleoceanographic changes in the Nordic Seas, *Paleoceanography*, 18 (1), 1017, 2003.
- 15 Risebrobakken, B., Dokken, T., Smedsrud, L. H., Andersson, C., Jansen, E., Moros, M. and Ivanova, E.: Early Holocene temperature variability in the Nordic Seas: the role of oceanic heat advection versus changes in orbital forcing, *Paleoceanography*, 26, 2011.
- Robbins, J. A. and Edgington, D. N.: Determination of recent sedimentation rates in Lake Michigan using Pb-210 and Cs-137, *Geochim. Cosmochim. Ac.*, 39, 285–304, 1975.
- 20 Rosenthal, Y., Lohmann, G. P., Lohmann, K. C. and Sherrell, R. M.: Incorporation and preservation of Mg in Globigerinoides sacculifer: Implications for reconstructing the temperature and  $^{18}\text{O}/^{16}\text{O}$  of seawater, *Paleoceanography*, 15(1), 135–145, 2000.
- Rögl, F. and Bolli, H. M.: Holocene to Pleistocene planktonic foraminifera, leg 15, site 147 (Cariaco Basin Trench Caribbean Sea) and their climate interpretation, In: Edgar, N.Y.,  
 25 Saunders, J.B. et al. (Eds), Initial reports of the Deep Sea Drilling Project, 15, 553–615, 1973.
- Rudels, B.: The thermohaline circulation in the Arctic Ocean and in the Greenland Sea, *Philos. Trans. R. Soc. Lond.*, A352, 287–299, 1995.
- Russell, A. D., Hönisch, B., Spero, H. J. and Lea, D. W.: Effects of seawater carbonate ion concentration and temperature on shell U, Mg, and Sr in cultured planktonic foraminifera,  
 30 *Geochim. Cosmochim. Ac.*, 68, 4347–4361, 2004.
- Saito, T., Thompson, P. R. and Breger, D.: Systematic index of recent and pleistocene planktonic foraminifera, University of Tokyo press, Tokyo, 1981.

Sakshaug, E. and Slagstad, D.: Sea ice and wind: Effects on primary productivity in the Barents Sea, *Atmosphere-Ocean*, 30, 579-591, 1992.

Sarnthein, M. and Werner, K.: Early Holocene planktic foraminifers record species-specific  $^{14}\text{C}$  reservoir ages in Arctic Gateway, *Mar. Micropaleontol.*, (135), 45–55, 2017.

5 Schiebel, R. and Hemleben, C.: Modern planktic foraminifera, *Paläontologische Zeitschrift*, 79, 135–148, 2005.

Schiebel, R., Spielhagen, R. F., Garnier, J., Hagemann, J., Howa, H., Jentzen, A., Martínez-García, A., Meilland, J., Michel, E., Repschläger, J., Salter, I., Yamasaki, M. and Haug, G.: Modern planktic foraminifers in the high-latitude ocean, *Mar. Micropaleontol.*, 136, 1–13,  
10 2017.

Schröder, W.: Case Studies on the Spörer, Maunder, and Dalton Minima, Science Edition, Bremen, 2005.

Shackleton, N. J.: Attainment of isotopic equilibrium between ocean water and the benthonic foraminifera genus *Uvigerina*: Isotopic changes in the ocean during the last glacial, *Centre  
15 National de la Recherche Scientifique Colloques Internationaux*, 219, 203–209, 1974.

Shindell, D. T., Schmidt, G., Miller, R. I. and Mann, M. E.: Volcanic and solar forcing of climate change during the preindustrial era, *J. Clim.*, 16, 4094–4107, 2003.

Simstich, J., Sarnthein, M. and Erlenkeuser, H.: Paired delta 18O signals of *Neogloboquadrina pachyderma* (s) and *Turborotalita quinqueloba* show thermal stratification  
20 structure in Nordic Seas, *Mar. Micropaleontol.*, 48, 107–125, 2003.

Smith, W. O. and Sakshaug, E.: Polar Phytoplankton, Part B, Chemistry, Biology and Geology, In: Smith Jr., W.O. (Ed.), Academic Press, New York, 477–525, 1990.

Spero, H. J., Bijma, J., Lea, D. W. and Bemis, B. E.: Effect of seawater carbonate concentration on foraminiferal carbon and oxygen isotopes, *Nature*, 390, 497–500, 1997.

25 Spielhagen, R. F., Werner, K., Aagaard-Sørensen, S., Zamelczyk, K., Kandiano, E., Budeus, G., Husum, K., Marchitto, T. and Hald, M.: Enhanced modern heat transfer to the Arctic by warm Atlantic water, *Science*, 331, 450, 2011.

Spielhagen, R. F. and Erlenkeuser, H.: Stable oxygen and carbon isotopes in planktic foraminifers from the Arctic ocean surface sediments: reflection of the low salinity surface  
30 water layer, *Mar. Geol.*, 119, 227–250, 1994.

Steinhilber, F., Abreu, J. A., Beer, J., Brunner, I., Christl, M. et al.: 9,400 years of cosmic radiation and solar activity from ice cores and tree rings, *Proceed. Nat. Acad. Sci. U.S.A.*, 109(16), 5967–5971, 2012.

- Stuiver, M. and Reimer, P. J.: Extended 14C data base and revised CALIB 3.0 14C age calibration program, In Stuiver, M., Long, A. and Kra, R.S., eds., Calibration 1993, Radiocarbon, 35(1), 215–230, 1993.
- Sutton, R. and Hodson, D.: Atlantic Ocean forcing of North American and European summer climate, Science, 309, 115–118, 2005.
- Telesiński, M. M., Przytarska, J. E., Sternal, B., Forwick, M., Szczuciński, W., Łącka, M. and Zajączkowski, M.: Palaeoceanographic evolution of the SW Svalbard shelf over the last 14 000 years, Boreas, 47, 410–422, 2018.
- Telford, R. J. and Birks, H. J. B.: The secret assumption of transfer functions: problems with spatial autocorrelation in evaluating model performance, Quat. Sci. Rev., 24, 2173–2179, 2005.
- Tinner, W., Beer, R., Bigler, C., Clegg, B. F., Jones, R. T., Kaltenrieder, P., van Raden, U. J., Gilli, A. and Hu, F. S.: Late-Holocene climate variability and ecosystem responses in Alaska inferred from high-resolution multiproxy sediment analyses at Grizzly Lake, Quat. Sci. Rev., 126, 41–56, 2015.
- Walczowski, W., Beszczyńska-Möller, A., Wieczorek, P., Merchel, M. and Grynczel, A.: Oceanographic observations in the Nordic Sea and Fram Strait in 2016 under the IO PAN long-term monitoring program AREX, Oceanologia, 59, 187–194, 2017.
- Vare, L. L., Massé, G. and Belt, S. T.: A biomarker-based reconstruction of sea ice conditions for the Barents Sea in recent centuries, The Holocene, 20(4), 637–643, 2010.
- Werner, K., Spielhagen, R. F., Bauch, D., Hass, H. C., Kandiano, E. and Zamelczyk, K.: Atlantic Water advection to the eastern Fram Strait- Multiproxy evidence for late Holocene variability, Palaeogeogr., Palaeoclim., Palaeoecol., 308(3–4), 264–276, 2011.
- Werner, K., Müller, J., Husum, K., Spielhagen, R. F., Kandiano, E. S. and Polyak, L.: Holocene sea subsurface and surface water masses in the Fram Strait-Comparisons of temperature and sea-ice reconstructions, Quat. Sci. Rev., 147, 194–209, 2016.
- Werner, J. P., Divine, D. V., Ljungqvist, F. Ch., Nilsen, T. and Francus, P.: Spatio-temporal variability of Arctic summer temperatures over the past two millennia: an overview of the last major climate anomalies, Clim. Past, 14, 527–557, 2017.
- Winkelmann D. and Knies, J.: Recent distribution and accumulation of organic carbon on the continental margin west off Spitsbergen, Geochem., Geophys., Geosys., 6, Q09012, 2005.

- Van Nieuwenhove, N., Hillaire-Marcel, C., Bauch, H. A. and de Vernal, A.: Sea surface density gradients in the Nordic Seas during the Holocene as revealed by paired microfossil and isotope proxies, *Paleoceanography*, 31, 380–398, 2016.
- Vinther, B. M., Jones, P. D., Briffa, K. R., Clausen, H. B., Andersen, K. K., Dahl-Jensen, D. and Johnsen, S. J.: Climatic signals in multiple highly resolved stable isotope records from Greenland, *Quat. Sci. Rev.*, 29, 522–538, 2010.
- Vinje, T. E.: Anomalies and trends of sea-ice extent and atmospheric circulation in the Nordic Seas during the period 1864–1998, *J. Clim.*, 14, 255–267, 2001.
- Vinje, T. E.: Sea ice conditions in the European sector of the marginal seas of the Arctic, 1966–75, Norwegian Polar Institute, 1975, 163–174, 1977.
- Volkman, R.: Planktic foraminifer ecology and stable isotope geochemistry in the Arctic Ocean: implications from water column and sediment surface studies for quantitative reconstructions of oceanic parameters, *Berichte zur Polarforschung*, 361, 1–128, 2000.
- Volkman, R. and Mensch, M.: Stable isotope composition ( $\delta^{18}\text{O}$ ,  $\delta^{13}\text{C}$ ) of living planktic foraminifers in the outer Laptev Sea and the Fram Strait, *Mar. Micropaleontol.*, 42, 163–188, 2001.
- Zamelczyk, K., Rasmussen, T., Husum, K., Haflidason, H., de Vernal, A., Krogh Ravna, E., Hald, M. and Hillaire-Marcel, C.: Paleoceanographic changes and calcium carbonate dissolution in the central Fram Strait during the last 20 ka, *Quat. Sci. Res.*, 78, 405–416, 2012.
- Zamelczyk, K., Rasmussen, T., Husum, K. and Hald, M.: Marine calcium carbonate preservation vs. climate change over the last two millennia in the Fram Strait: implications for planktic foraminiferal paleostudies, *Mar. Micropaleontol.*, 98, 14–27, 2013.
- Zamelczyk, K., Rasmussen, T., Husum, K., Godtliessen, F. and Hald, M.: Surface water conditions and calcium carbonate preservation in the Fram Strait during marine isotope stage 2, 28.8–15.4 kyr, *Paleoceanography*, 29, 1–12, 2014.

**Table 1** AMS<sup>14</sup>C and calibrated dates in core HH12-1206BC.

Lab nr	Depth (cm)	Age <sup>14</sup> C BP	Calibrated yr BP	δ <sup>13</sup> C	Age AD/BC
Poz-59603	2–3.5	520 ± 80*	1–279	–3.9	~1949–1671
Poz-102419	4.5–6.5	460 ± 40*	160–198	–22.6	1752–1790
Poz-57342	9.5–11.5	900 ± 80*	357–644	–16.2	1306–1593
Poz-102418	13–14	580 ± 35	94–292	–4.1	1658–1856
Poz-66095	14–16	830 ± 110	258–634	–14.6	1316–1692
Poz-59605	19–20	1175 ± 30	652–779	0.3	1171–1298
Poz-102417	22–22.5	1515 ± 30	966–1158	–2.6	792–984
Poz-66211	23.5–25	1870 ± 70	1272–1560	–17.6	390–678
Poz-57343	30–31	2320 ± 80	1724–2132	–4.3	183BC–226

\*Date not used in age model.

**Table 2** Compilation of vital effects reported from the Fram Strait in the literature for *Neogloboquadrina pachyderma* and *Turborotlita quinqueloba* and references.

<i>N. pachyderma</i>		<i>T. quinqueloba</i>		Reference
δ <sup>18</sup> O (‰)	δ <sup>13</sup> C (‰)	δ <sup>18</sup> O (‰)	δ <sup>13</sup> C (‰)	
–1.5	–2.6	–3.7	–3.6	Pados et al. (2015)
0	–	–0.7	–	Jonkers et al. (2010)
–1	–0.85	–1.1	–2	Simstich et al. (2003)
–1.6	–2.1	–1.3	–2.6	Volkman and Mensch (2001)
–0.9	–1	–1.2	–2.2	Stangeew (2001)

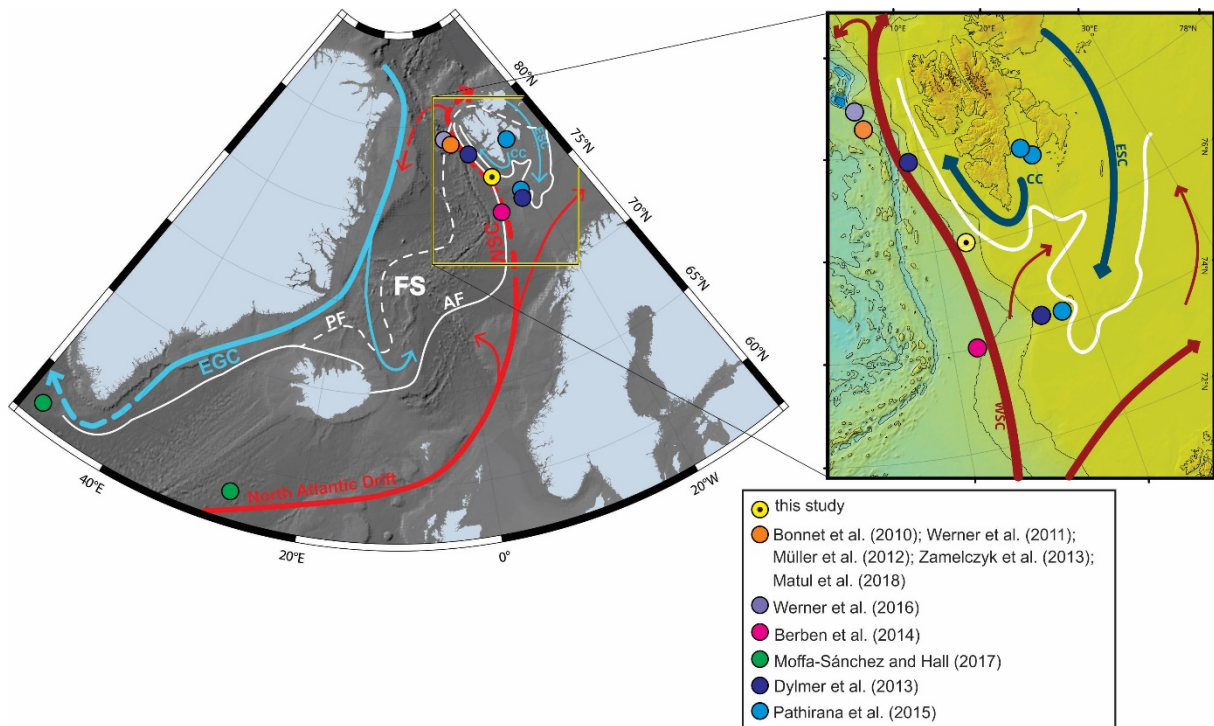


**Figure 1**

**Left panel:** Schematic map of the northern North Atlantic, the Fram Strait and the western Barents Sea showing bathymetry, present-day surface currents and average position of the Polar and Arctic fronts (based on Marnela et al. 2008). **Right panel:** Close-up of the northern continental margin off Svalbard and the north-western Barents Sea. The solid and dashed lines indicate surface and subsurface currents, respectively. Location of core HH12-1206BC (yellow circle) is indicated. Abbreviations: FS: Fram Strait; WSC: West Spitsbergen Current; CC: Coastal Current; ESC: East Spitsbergen Current; EGC: East Greenland Current; AF: Arctic Front; PF: Polar Front. Locations of published records discussed in the text are marked and listed in the legend.

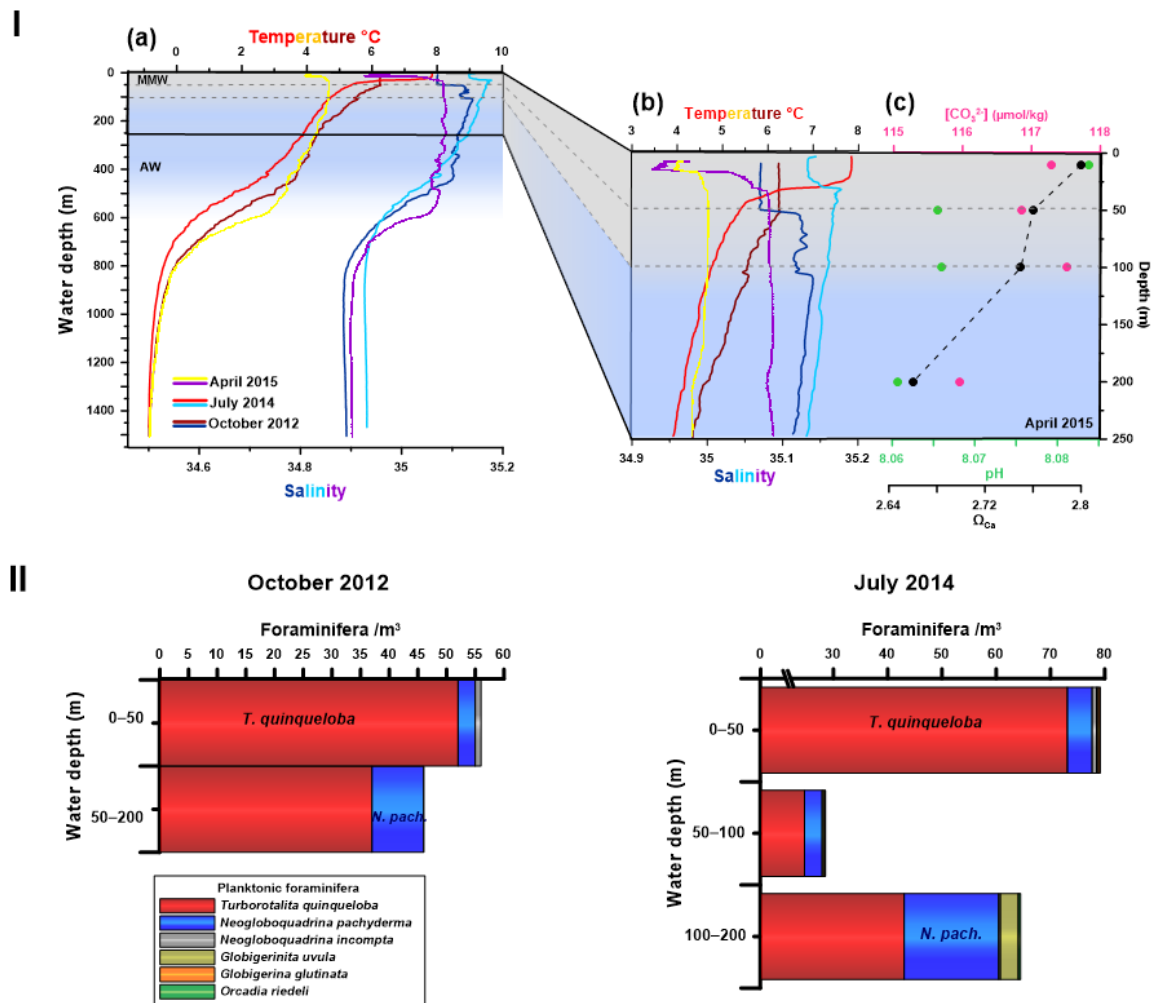


**Figure 2**

I: (a) Conductivity-temperature-depth (CTD) profile showing water mass distribution of the water column in October 2012, July 2014 and April 2015 at site HH12-1206BC; (b) close-up of CTD data in upper 250 m; (c) carbonate ion concentration  $[\text{CO}_3^{2-}]$ , calcium carbonate saturation state ( $\Omega_{\text{Ca}}$ ) and pH in upper 250 m in April 2015. II: Distribution of planktic foraminifera in the water column in October 2012 and July 2014. Abbreviations: MMW, mixed melt water; AW, Atlantic water.

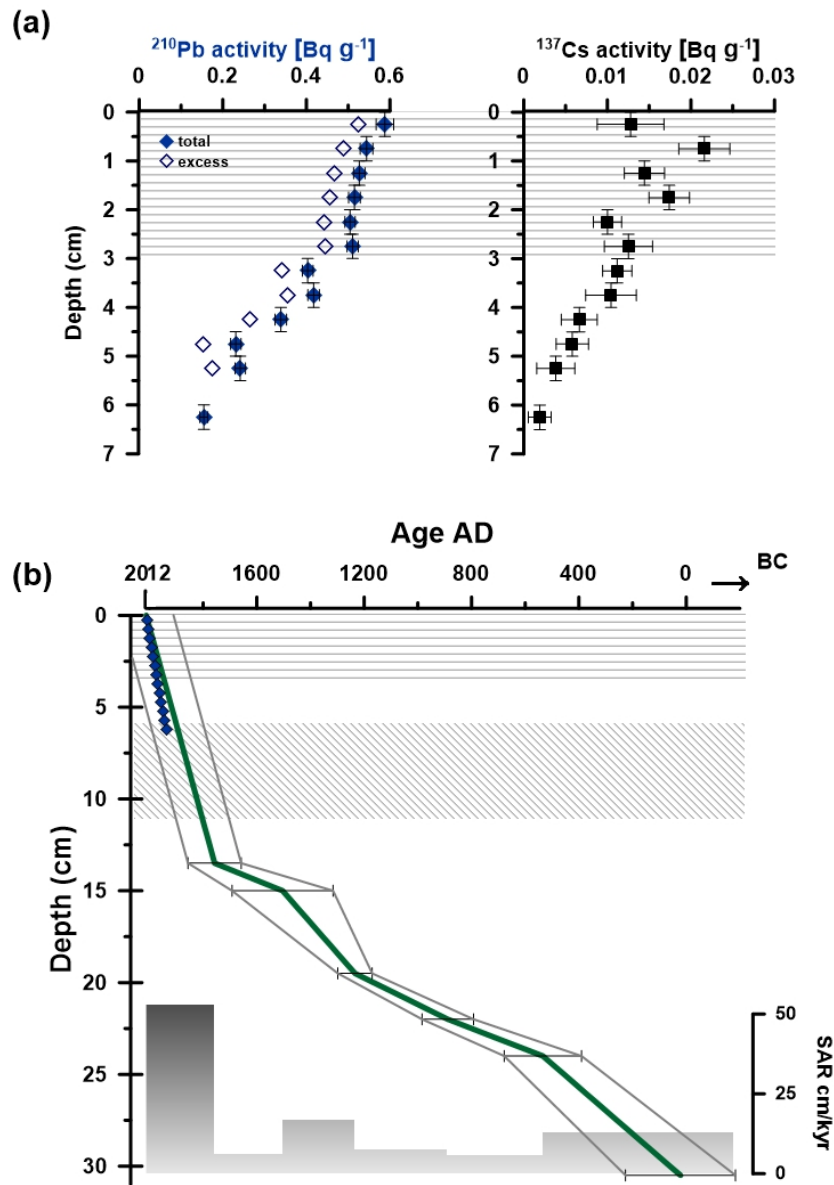


**Figure 3**

Age model based on  $^{210}\text{Pb}$ ,  $^{137}\text{Cs}$  and AMS  $^{14}\text{C}$  datings in core HH12-1206BC: (a) total and excess  $^{210}\text{Pb}$  activity profiles and  $^{137}\text{Cs}$  activity profile. In (a) vertical bars indicate sampling range, whereas horizontal bars mark  $2\sigma$  uncertainties. In (b) error bars of AMS dates represent  $2\sigma$  standard deviation and are indicated by grey-lined field, and dark blue diamonds indicate the age model based on  $^{210}\text{Pb}$  activity. The area with horizontal lines in (a) and (b) represent mixing of sediment in the upper 3 cm indicated by  $^{210}\text{Pb}$  activity profiles. In (b) dashed area shows interval of reversed  $^{14}\text{C}$  dates. Sedimentation rate is shown at the bottom of panel (b).

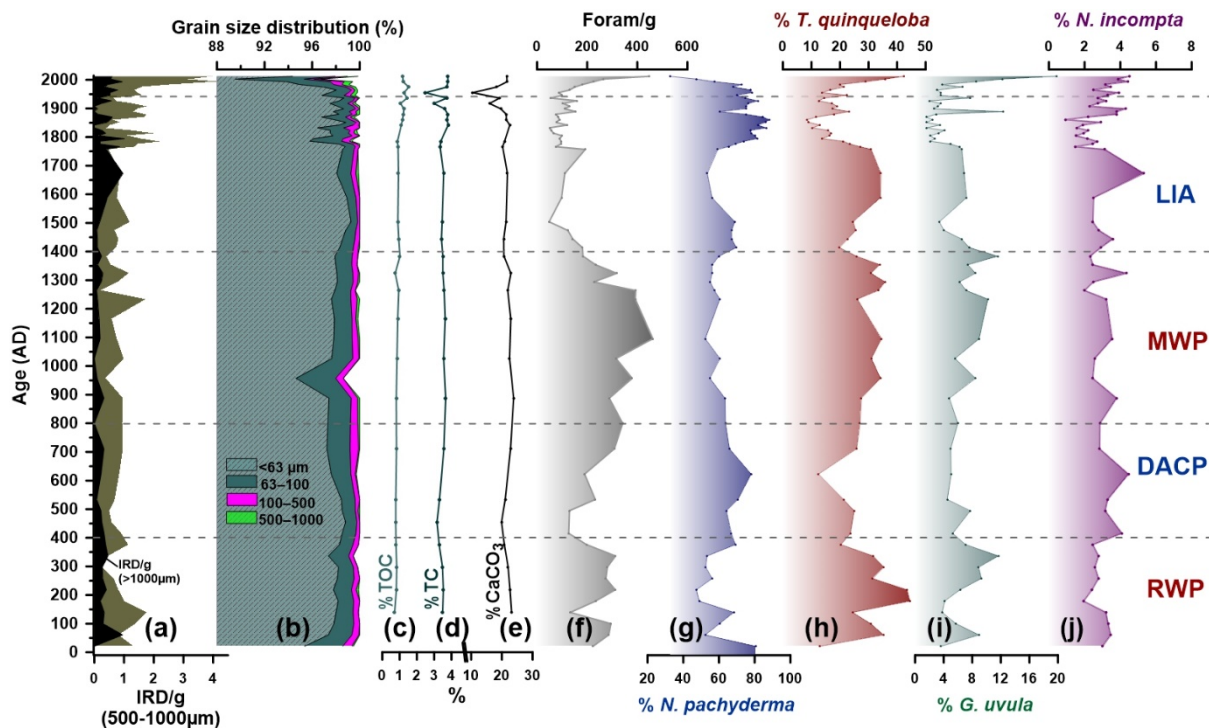


**Figure 4**

Grain size distribution, geochemical and foraminiferal records plotted versus age in core HH12-1206BC. (a) concentration of IRD in number per g dry weight sediment, (b) % cumulative diagram of grain size distribution, (c) % TOC, (d) % TC, (e) % CaCO<sub>3</sub>, (f) concentration of planktic foraminifera in number per g dry weight sediment, and relative abundance of (g) *Neogloboquadrina pachyderma*, (h) *Turborotalita quinqueloba*, (i) *Globigerinita uvula*, (j) *N. incompta*. Abbreviations: RWP, Roman Warm Period; DACP, Dark Ages Cold Period; MWP, Medieval Warm Period; LIA, Little Ice Age.

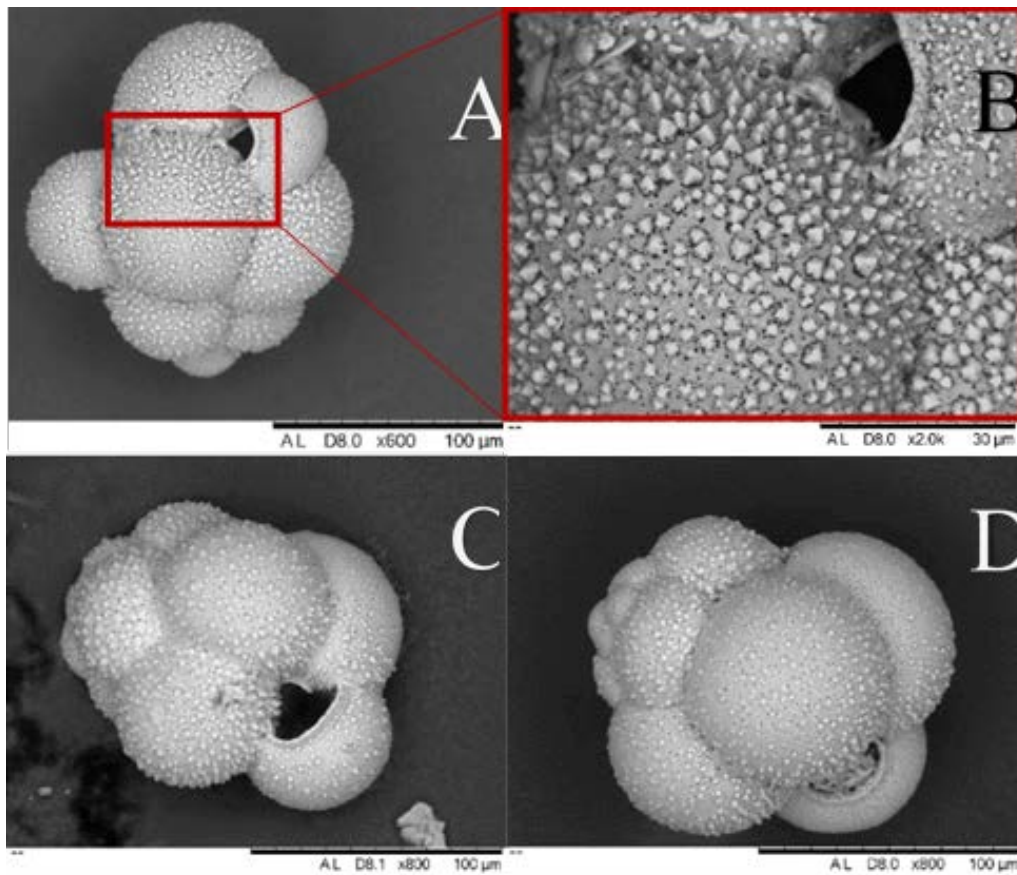


**Figure 5**

SEM pictures of planktic foraminiferal species *Globigerinita uvula minuta* (Natland, 1938) in core HH12-1206BC. A, B) 9.5–10 cm, C) 7.5–8 cm, D) 11–11.5 cm down core. This form is similar to *Globigerinita uvula*, but significantly larger, with strongly inflated chambers and comparatively low trochospiral test. Similar to *G. uvula* it possesses a smooth, finely perforated wall, but with stronger encrustations of crystalline knobs (Rögl and Bolli, 1973) (B).

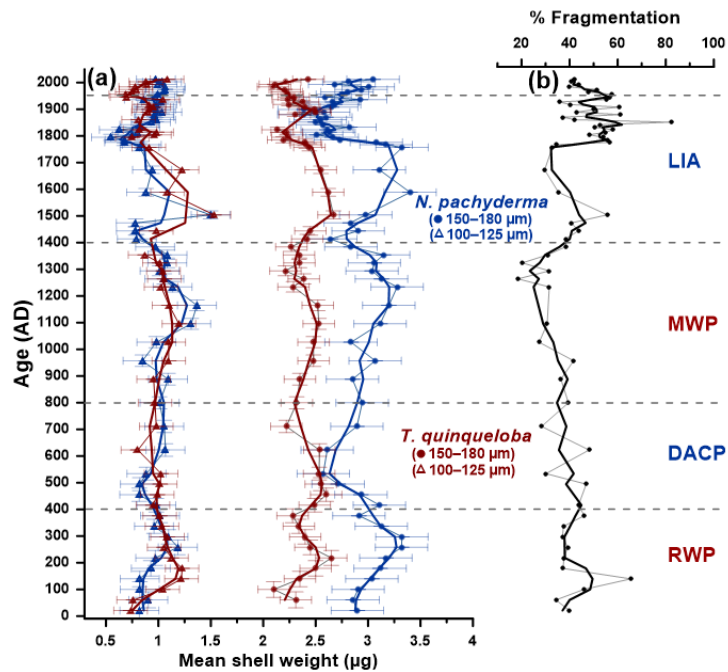


**Figure 6**

(a) Mean shell weight of planktic foraminiferal species *Neogloboquadrina pachyderma* and *Turborotalita quinqueloba* in size-fraction 100–125  $\mu\text{m}$  and 150–180  $\mu\text{m}$ , (b) % fragmentation of planktic shells in core HH12-1206BC. Thick lines indicate 3-point moving average and horizontal bars mark standard deviation.

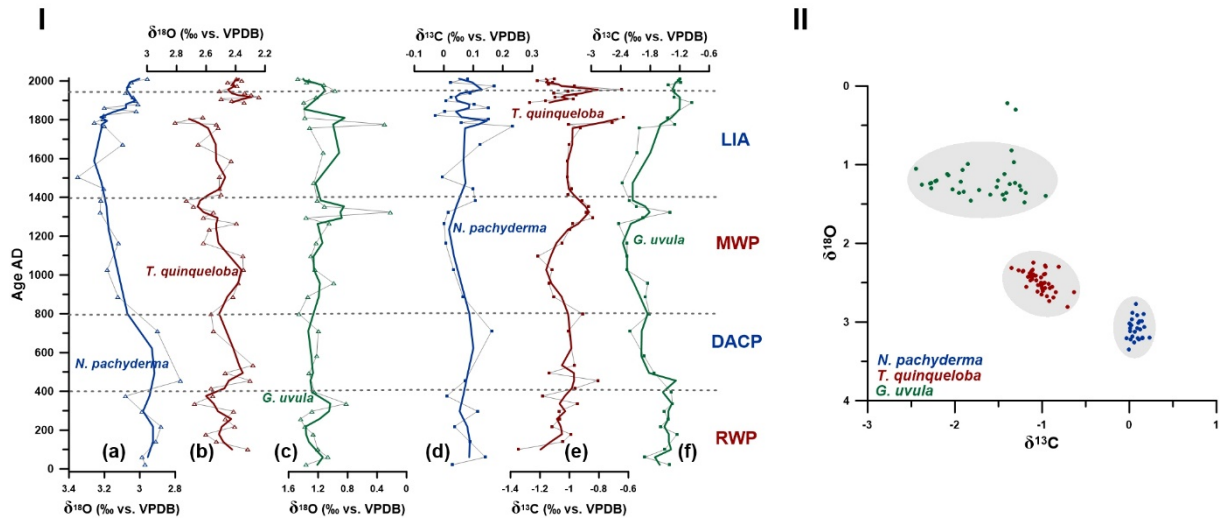


**Figure 7**

Stable isotope records (raw data) in core HH12-1206BC. I:  $\delta^{18}\text{O}$  and  $\delta^{13}\text{C}$  of (a,d) *Neogloboquadrina pachyderma*, (b,e) *Turborotalita quinqueloba* and (c, f) *Globigerinita uvula*, respectively. Thick lines represent 3-point moving averages. II: Oxygen versus carbon isotope plot of *N. pachyderma*, *T. quinqueloba* and *G. uvula*.

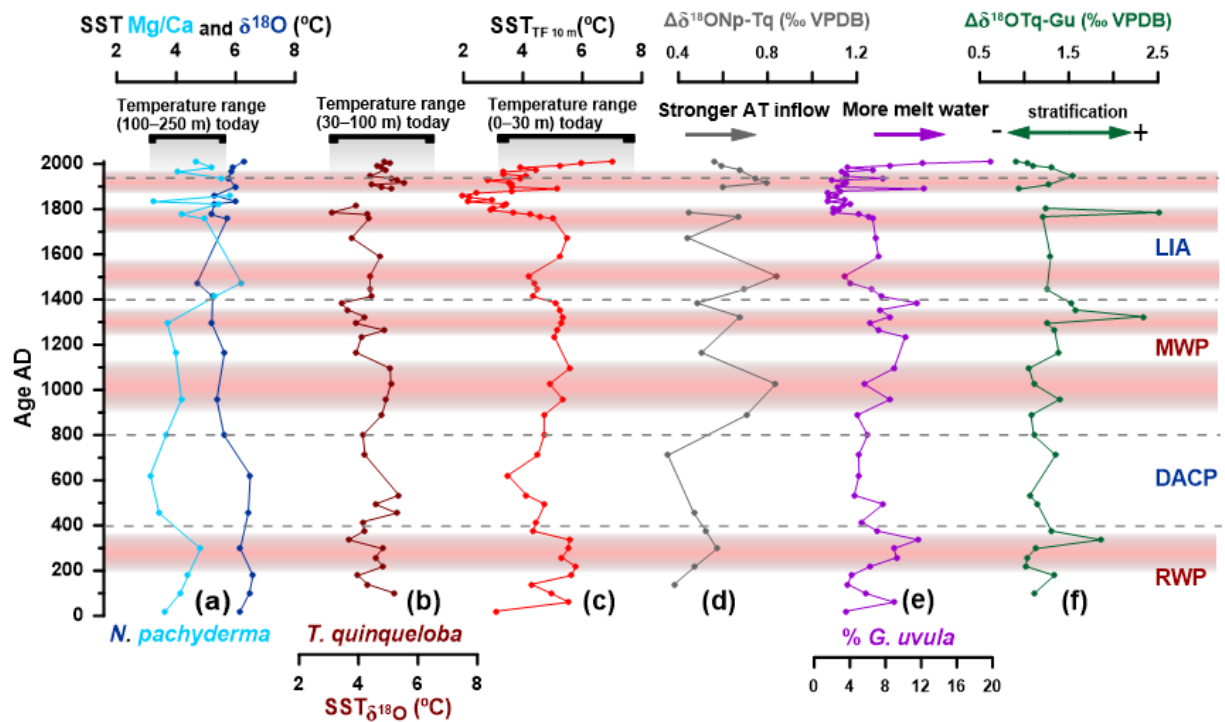


**Figure 8**

Comparison of reconstructed SST plotted versus age in core HH12-1206BC. (a)  $\delta^{18}\text{O}$  and Mg/Ca ratio based SST on *N. pachyderma*, (b)  $\delta^{18}\text{O}$  based SST on *T. quinqueloba*, (c) transfer function based  $\text{SST}_{\text{TF}}$  at 10 m water depth, (d)  $\Delta\delta^{18}\text{O}_{\text{Np-Tq}}$  as an indicator of stronger Atlantic Water inflow (e) % *G. uvula* as a proxy for supply of meltwater, and (f)  $\Delta\delta^{18}\text{O}_{\text{Tq-Gu}}$  as an indicator of relative changes in stratification of near surface and surface water. Gray bars on top represent present day temperature ranges at 100–250 m, 30–100 m and 0–30 m water depth. Red bars indicate periods of stronger Atlantic Water inflow accompanied by increased presence of meltwater and enhanced stratification of the subsurface, near surface and surface water masses.

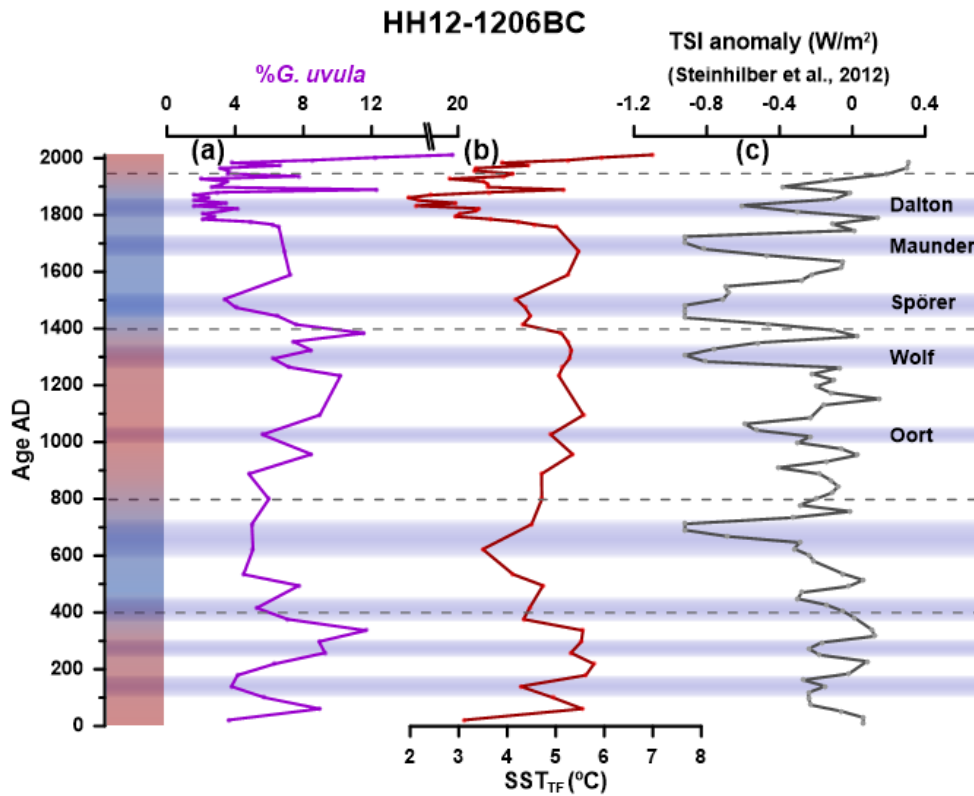


**Figure 9**

Comparison of (a) % of *G. uvula*, (b) SST<sub>TF</sub> in core HH12-1206BC to (c) TSI anomalies with solar minima (Steinhilber et al., 2012) of the last two millennia. Known solar minima during the last 1000 years; Oort (1010–1050 AD), Wolf (1280–1350 AD), Spörer (1460–1550 AD), Maunder (1645–1715 AD) and Dalton (1790–1820 AD) (Eddy, 1978; Schröder, 2005) are indicated. Left panel shows warm (red) and cold (blue) climatic periods during the past 2000 years.